3

Manufacture of polyester fibres

C. A. LIN, Feng Chia University, Taiwan

3.1 Introduction

Polyethylene terephthalate (PET) is a linear polyester consisting of organic compounds of repeating ester groups (–COO–). The usefulness of polyester for fibres was discovered when terephthalate acid was incorporated into the repeat unit of the polymer molecule. The PET textiles made possible the increasingly wider applications of synthetic fibres due to the outstanding physical and chemical characteristics which polyester fibres possess in comparison with natural and synthetic fibres; such as, excellent dimensional stability and sturdiness, a high degree of crease resistance, good bulk elasticity, and warm handle. Further PET characteristics such as great stability of thermoset creases, a high degree of light and heat resistance, and durability of polyester textiles, due to their great fibre strength and elongation, are also very good. Finally, the care of polyester is facilitated by quick drying due to the low water sorption and their relatively good resistance to washing treatments and bacteria and microbes. As a result, mass production of PET fibres enhanced the manufacture of other synthetic fibres.

The use of terephthalic acid with ethylene glycol for the development of PET fibres is introduced as follows. Esterification results from the reaction of carboxylic acid with alcohols in the presence of heat and inorganic acid; such as H_2SO_4, in accordance with the following scheme:

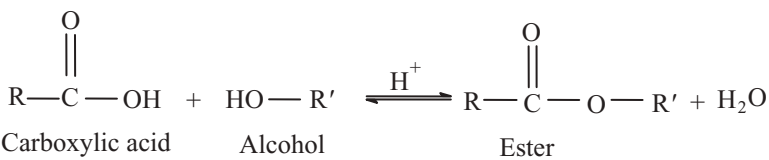

R may be alkyl or aryl R' is usually alkyl

During esterification, it is always necessary for a small molecule (e.g., water) to be rapidly removed from the reaction mixture. This is called a condensation reaction. When two functional compounds are used in a condensation reaction, they will produce a condensation polymer. In general, a polymer is formed from joining many molecules by condensation reaction. Almost any condensation reaction can be used to prepare polymers provided that the reaction is performed with monomers having two functional groups. For example, the reaction between a compound with two alcohol groups and a compound with two carboxylic acid groups forms a polymer. The polymers can be classified according to the chemical group linking the monomer units. Polyester is a polymer with repeating units linked by an ester group.

Polyester was first prepared in 1863. Bischoff made polyester from dihydric phenole and dicarboxylic acid in 1902. Fischer prepared polyester from *p*-hydroxyenzoic acid in 1908–1910.[1] Carothers[2] dealt with the condensation polymerisation and the structure of polyester. He was the first to produce spinnable polyester of high molecular weight by condensation reaction α, ω-diols with alkanedioic acids, or by condensation reaction ω-hydroxyalkanoic acids. Moreover, he published a series of papers about polyester in the period 1928 to 1929. Carothers[3] prepared a series of esters from aliphatic diols of formula $HO(CH_2)yOH$ and aliphatic dicarboxylic acids of formula $HOOC(CH_2)xCOOH$. The reaction proceeds as:

$$HOOC(CH_2)xCOOH + HO(CH_2)yOH \rightarrow -(OC(CH_2)xCOO(CH_2)yO)n- + 2n\ H_2O$$

where y was 2, 3, or 6 and x was 1, 2, 4, 8. The polyester was produced by alcoholysis; i.e., by heating glycol with oxalate, when alcohol was eliminated. The reaction is,

$$ROOC–COOR + HO(CH_2)xOH \rightarrow -(COO(CH_2)xOOC)n- + 2n\ ROH$$

where R was C_2H_5 or C_3H_7 and x was 10. Polyester produced by polymer/monomer interconversion such as the lactones of δ-hydroxyvaleric acid is shown below.

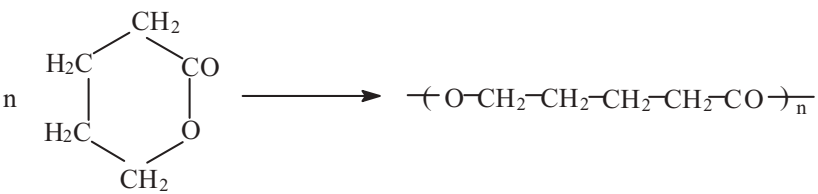

The ability of bifunctional lactones has been discussed by Carothers *et al.*[4] It was found that the five-membered ring systems stand out to be very stable. The six-membered ones can be converted into linear polyester and by proper treatment back to the monomeric form. Because of intermolecular reaction or intramolecular reaction, a bifunctional compound such as α-hydroxy acid may yield both diametric cyclic ester and a linear polyester.

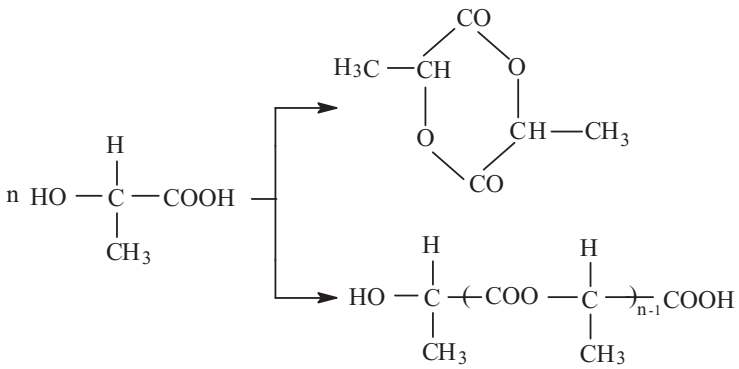

Cyclic esters with rings of six or more members can be depolymerised into linear polyester. In the reaction of a bifunctional compound, however, the probability that the chain takes up a configuration allowing the ends of the molecule to react is low. Moreover, such ring configurations will be few in number compared with all possible ones. The probability that the two ends of a long chain will occupy positions adjacent to one another, and hence be in a position to react intramolecularly, varies roughly as (chain length)$^{-3/2}$. As a result, intramolecular reactions become less probable as the number of atoms in the molecule increases.

The lactones of δ-hydroxyvaleric acid formed from the corresponding ω-hydroxy acid produce a linear polyester as follows:

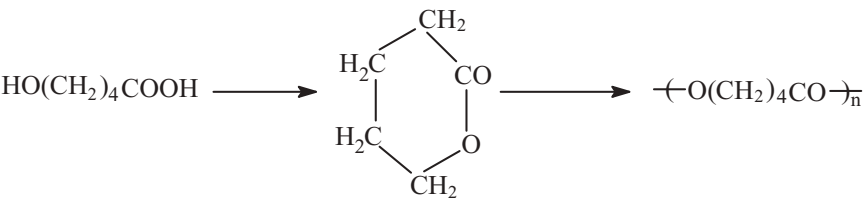

In polymer preparation, the compound with six-membered or beyond cyclic lactones is quite readily transformed to polymer. Carothers and Hill pro-

duced a polyester melt (m.p. 75°C) by polycondensation of ethylene glycol and sebacic acid. The polycondensation was carried out as part of a molecular distillation or simply by passing nitrogen through the condensation melt until a fibre-forming polyester resulted. The filaments were then processed by cold drawing. They also produced other fibre-forming polyesters; such as the reaction products from propylene glycol and hexadecane dicarboxylic (octadecanedivic) acid (m.p. 75°C), propylene glycol and ω-hydroxydecanoic acid (m.p. 65°C), and propylene glycol and ω-hydroxypentadecanoic acid (m.p. 95°C).

In 1931, Carothers produced a polyamide '66' or so-called 'nylon' from adipic acid and hexamethylene diamine. Further, Carothers and his collaborators found very large differences in melting points between polyesters and the corresponding polyamides. Polyester melt (m.p. 57°C) resulted from reaction of adipic acid with ethylene glycol, while a polyamide melt (m.p. 278°C) was produced by the reaction of adipic acid with tetramethylene diamine. Also, a polyester melt (m.p. 75°C) was formed by the reaction of sebacic acid with ethylene glycol, while a polyamide melt (m.p. 254°C) was produced by the reaction of sebacic acid with ethylene diamine. Because of the thermal stability and the fact that the melting points of the polyesters produced from aliphatic dicarboxylic acids and glycols were considerably lower than those of the corresponding polyamides, Carothers and his collaborators turned their attention to polyamides to exploit their discovery commercially.

In 1941, Schlack implemented terephthalic acid for the development polyester fibres in Germany at a branch of Agfa Wolfen. He focused more on producing polyester from terephthalic acid and 1, 4-butanediol (m.p. 218°C). At the same time, Whinfield and Dickson applied it at Calico Printers' Association in Great Britain,[5] while they preferred using a combination of terephthalic acid and ethylene glycol to produce polyester melt (m.p. 268°C). Both polyesters are crystalline and quite adequate for forming fibres. Nevertheless, from the point of view of economy and application to textile usage, the combination selected by Whinfield and Dickson was mostly preferred so that, industrially, the polyester fibres produced from terephthalic acid and ethylene glycol have maintained their competitive importance.

The relationship between the work of Carothers, Schlack, and Whinfield and Dickson is shown in the following diagrammatic representation:

$$\underset{\text{Dicarboxylic}}{HOOC{-}R_1{-}COOH} + \underset{\text{Glycol}}{HO{-}R_2{-}OH} \rightarrow$$

$$HO{-}\left(R_2{-}OOC{-}R_1{-}COO\right)_n R_2{-}OH$$

Polyester

Carothers $R_1 = -(CH_2)_8-$ (sebacic acid)

$R_2 = -(CH_2)_2-$ (ethylene glycol)

Schlack $R_1 =$ 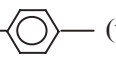 (terephthalic acid)

$R_2 = -(CH_2)_4-$ (1,4-butanediol)

Whinfield and Dickson $R_1 =$ 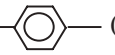 (terephthalic acid)

$R_2 = -(CH_2)_2-$ (ethylene glycol)

In 1947, mass production, based on the technological development of polyester fibres originated by Whinfield and Dickson, was conducted in Great Britain by Imperial Chemical Industries Ltd (ICI) and in America by the Du Pont de Nemours Company after both companies had acquired the patent rights from the Calico Printers' Association Ltd, in Manchester. ICI marketed polyester fibre as 'Terylene', whilst the fibre produced by Du Pont was called 'Dacron'. Then, the patent rights covering the polyester fibres developed by the Calico Printers' Association Ltd and ICI were made available to other firms in France, Italy, etc.

Fibre-forming polyester must possess the necessary properties (melting point, average molecular weight, dyeability, resistance to chemicals, etc.) so that it can be utilized commercially. Aliphatic polyester has low melting temperature;[6] examples are:

$$HO(CH_2)_9COOH \rightarrow \text{-}(O(CH_2)_9CO)_n\text{-} + H_2O$$

Properties of this polyester: crystallization, forming fibre, can be drawn at room temperature, and melting temperature is 76°C, and

$$HO(CH_2)_{10}OH + HOOC(CH_2)_4COOH \rightarrow$$
$$-(O(CH_2)_{10}OOC\ (CH_2)_4CO)n- + H_2O$$

Properties of this polyester: crystallization, forming fibre, can be drawn in room temperature, and melting temperature is 80°C.

Aromatic polyester has high melting temperature. The reaction is

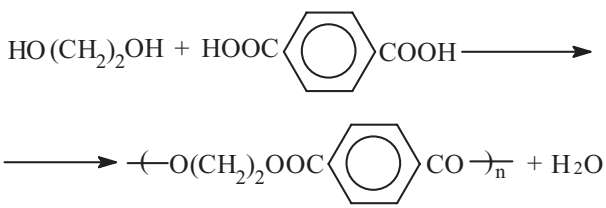

Properties of this polyester: rigid, crystallization, forming fibre, can be drawn in room temperature, and melting temperature is 264°C.

The clothing industry requires polyester of higher strength, greater crystallisation, higher resistance to light, etc. Thus, aromatic polyester of higher melting temperature is chosen for fibre production. In future, degradable fibres or green polymer is of great importance. Polyester has more thermal hydrolytic degradation, more alkaline degradation,[7] and thermal oxidative degradation.[8–9] Polyester is a chemical synthetic degradable polymeric material. In particular, the fibre-forming polyester with low melting temperature is the best material. Therefore, the aliphatic polyester may be selected for producing green polymer and degradable fibres.

3.2 Raw materials of polyester fibres in industry

The fibre-forming polyester may be obtained from dicarboxylic acids with diols, hydroxyl acids, or lactones. Commercially, aromatic polyester is applied using ethylene glycol (EG) and dimethyl terephthalate (DMT), or ethylene glycol and terephthalic acid (TPA) to produce polyethylene terephthalate (PET).

Before 1970, polyester was exclusively produced on a commercial scale from ethylene glycol and dimethyl terephthalate. After 1970, Mobil Co. and Amoco Co. were able to successfully develop technologies to produce pure terephthalic acid. Polyester then started to be produced from ethylene glycol with terephthalic acid. The refining processes for crude oil into ethylene, toluene and xylene are shown in Fig. 3.1.

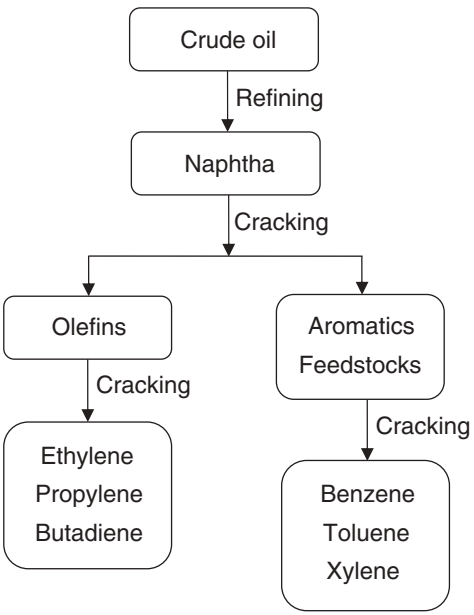

3.1 The refining processes for crude oil.

The producing processes of ethylene glycol, dimethyl terephthalate, and terephthalic acid are discussed in the following sections.

3.2.1 Production of ethylene glycol

Two methods have achieved importance for the manufacture of ethylene glycol including the ethylene oxide method and the ethylene chlorohydrin method.

Ethylene oxide method

Ethylene passes through oxidation processes to produce ethylene oxide which is then hydrated to form ethylene glycol. This method is achieved by:

(a) Producing ethylene oxide from ethylene
Direct oxidation and chlorine processes are of great importance for the technical manufacturing of ethylene oxide.
(i) Direct oxidation process
This process involves direct oxidation of ethylene to ethylene oxide[5] according to the following reaction

$$CH_2{=}CH_2 + \frac{1}{2}O_2 \xrightarrow[\text{Catalysts,150~300°C}]{\text{Oxidation}} H_2C\!-\!CH_2 \quad (\text{O bridge})$$

The reaction uses metal catalysts (e.g., silver oxide) and the reaction temperature is approximately 250°C.

(ii) Chlorine process
The chlorine process is carried out in two stages. In the first stage, ethylene with hypochlorous acid is transformed into ethylene chlorohydrin.

$$CH_2 = CH_2 + HOCl \xrightarrow[H_2O]{Cl_2} HOCH_2{-}CH_2Cl$$

In the second stage, ethylene chlorohydrin along with calcium hydroxide produces ethylene glycol.

$$2HOCH_2{-}CH_2Cl \xrightarrow{Ca(OH)_2} 2\,CH_2{-}CH_2\ (\text{O bridge}) + CaCl_2 + 2\,H_2O$$

(b) Production of ethylene glycol from ethylene oxide
Ethylene oxide may react with water and be hydrated to ethylene glycol in accordance with the following reaction[10]

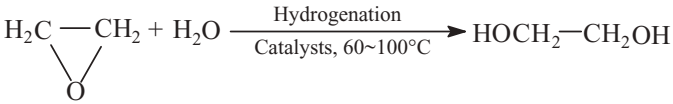

The reaction proceeds with the aid of acid catalysts, while the reaction temperature ranges between 60 to 100°C.

Ethylene chlorohydrin method

Ethylene glycol is produced by alkaline saponification of ethylene chlorohydrin with caustic soda solution, or of ethylene chloride and soda according to the following formulae:

$$ClCH_2–CH_2OH + H_2O \xrightarrow{\text{Caustic soda}} HOCH_2–CH_2OH + HCl$$

$$ClCH_2–CH_2Cl + 2H_2O \xrightarrow{\text{Soda}} HOCH_2–CH_2OH + 2HCl$$

However, this method is one of the older procedures and thus it was abandoned. Ethylene glycol was purified to produce polyester fibres with the following properties:

- Boiling point: 195–198°C.
- Density: 1.110–1.112 (at 20°C).
- OH number: greater than 1750.
- Water content: less than 0.1%.
- Ester interchange value: greater than 90.

3.2.2 Manufacturing terephthalic acid and dimethyl terephthalate

Benzene, toluene and xylene are the primary raw materials in manufacturing terephthalic acid and dimethyl terephthalate. The flow chart for the manufacturing processes of TPA and DMT is depicted in Fig. 3.2.

Benzene material

The following reaction system shows the conversion of benzene to terephthalic acid:

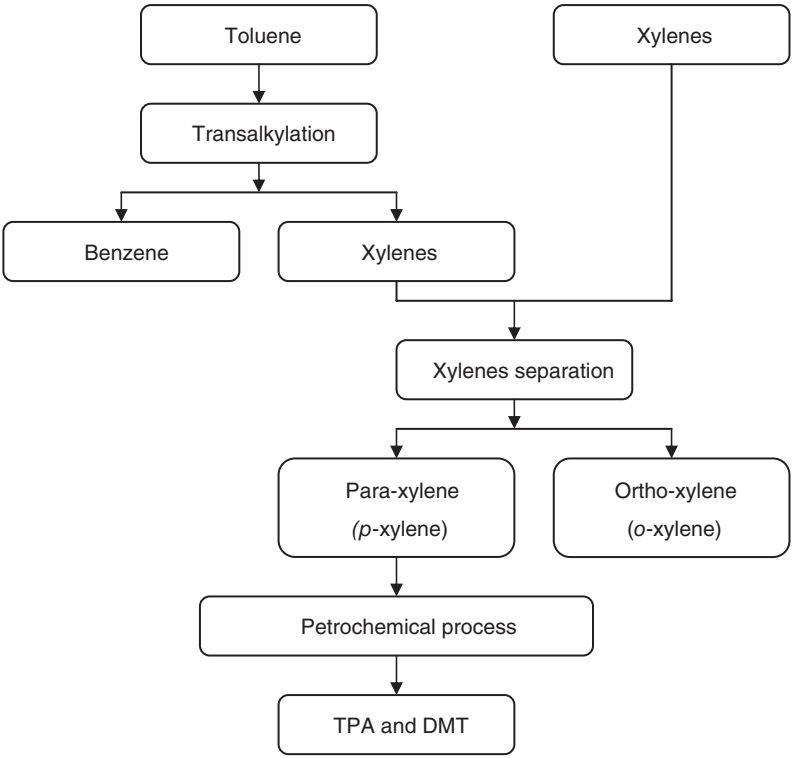

3.2 Flow chart for TPA and DMT.

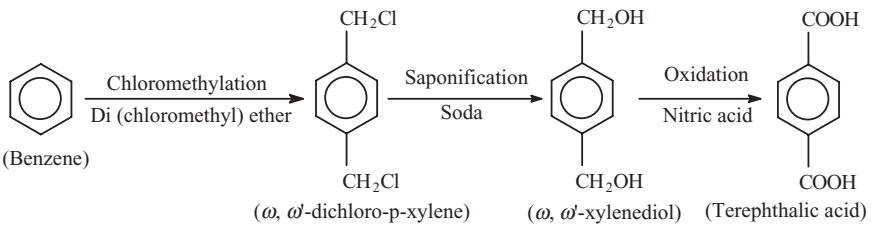

or

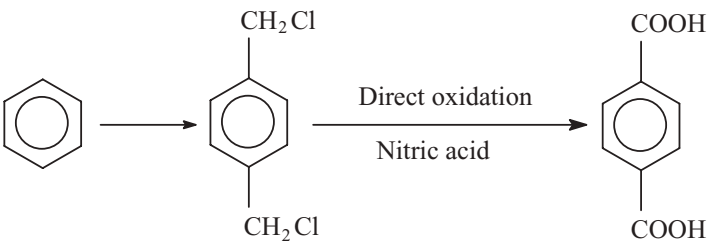

Toluene material

Four major processes of manufacturing terephthalic acid and dimethyl terephthalate from toluene including:

1. Synthesis via *p*-tolualdehyde
   The synthesis produces terephthalic acid and dimethyl terephthalate according to the following reaction patterns:

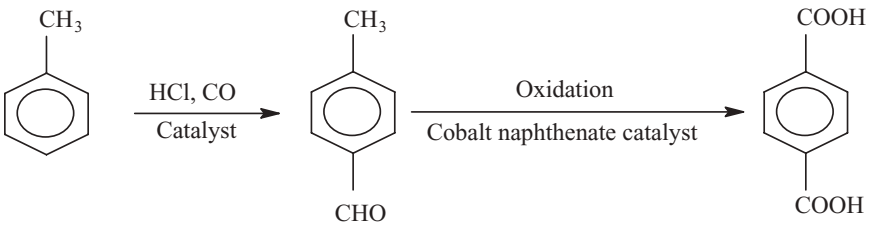

(Toluene) (p-tolualdehyde)

or

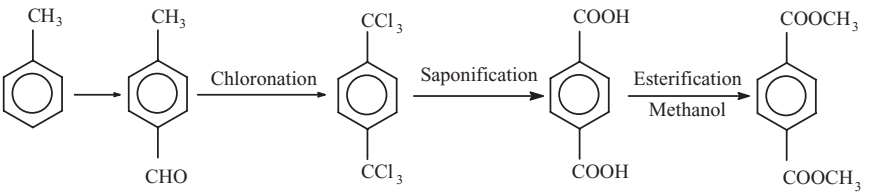

(Dimethyl terephthalate)

2. Synthesis via ω, ω′-dichloro-*p*-xylene
   The terephthalic acid or dimethyl terephthalate is obtained by three established processes according to the following formulae:

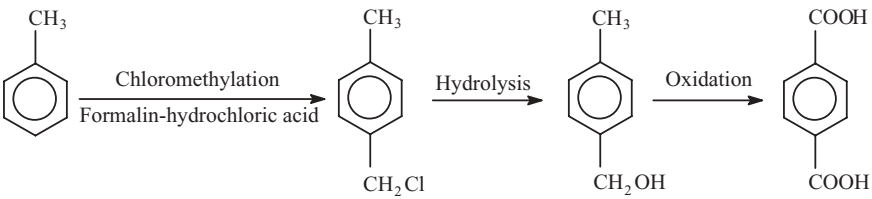

(ω-chloro-xylene) (4-methylbenzyl alchohol)

or

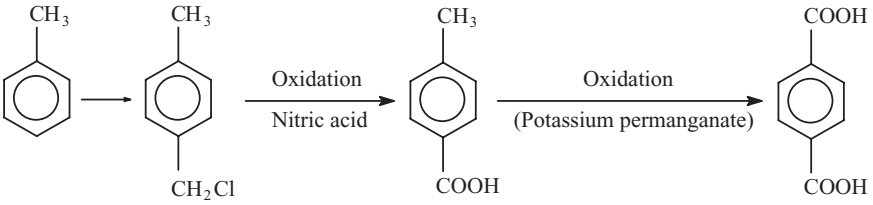

(p-toluic acid)

or

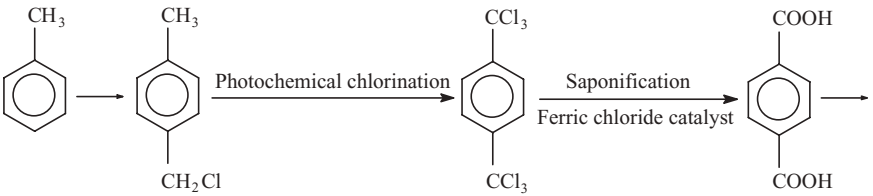

(Hexachloro-p-xylene)

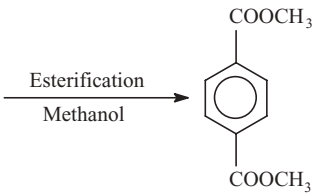

3. Synthesis via *p*-toluamide
   The manufacture of terephthalic acid based on tolune proceeds as follows:

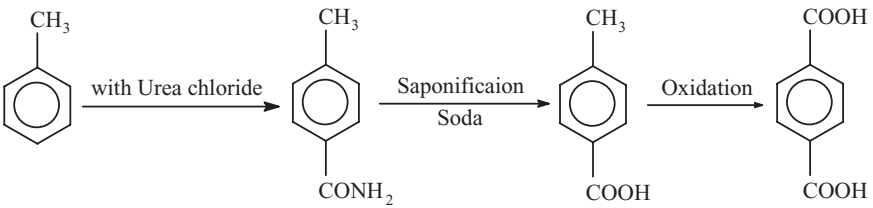

(p-toluamide)

4. Synthesis via potassium benzoate
   The synthesis for the production of terephthalic acid is based on the following reactions:[11]

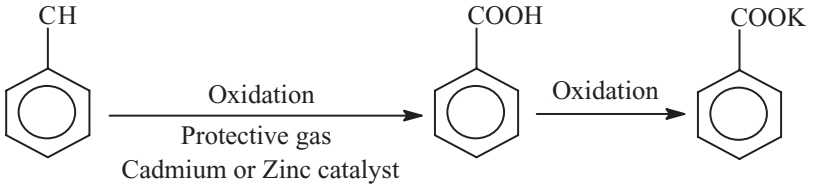

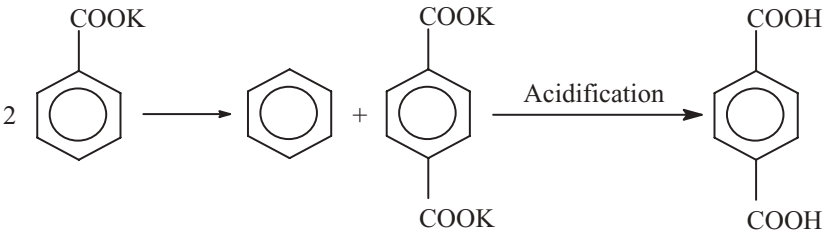

Material from p-*xylene*

Conversion of *p*-xylene mainly occurs by oxidation. Terephthalic acid and dimethyl terephthalate are produced from *p*-xylene according to the following formula:

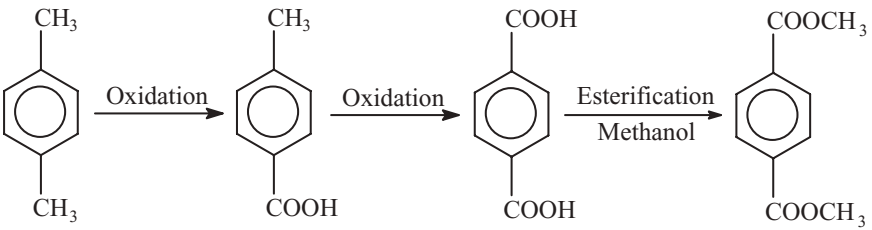

The oxidation of *p*-xylene may be carried out in two ways:

(a) One-step oxidation process, which includes catalytic oxidation,[12] and the Willgerodt reaction,[13] etc.
(b) Two-step oxidation process,[14] which leads directly to dimethyl terephthalate by the following reaction:

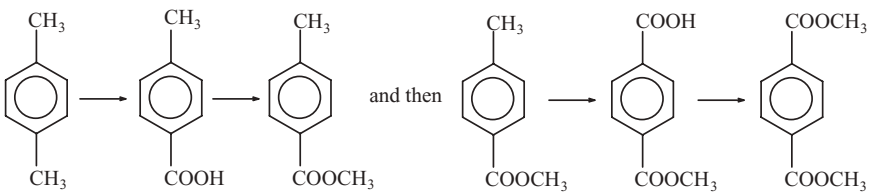

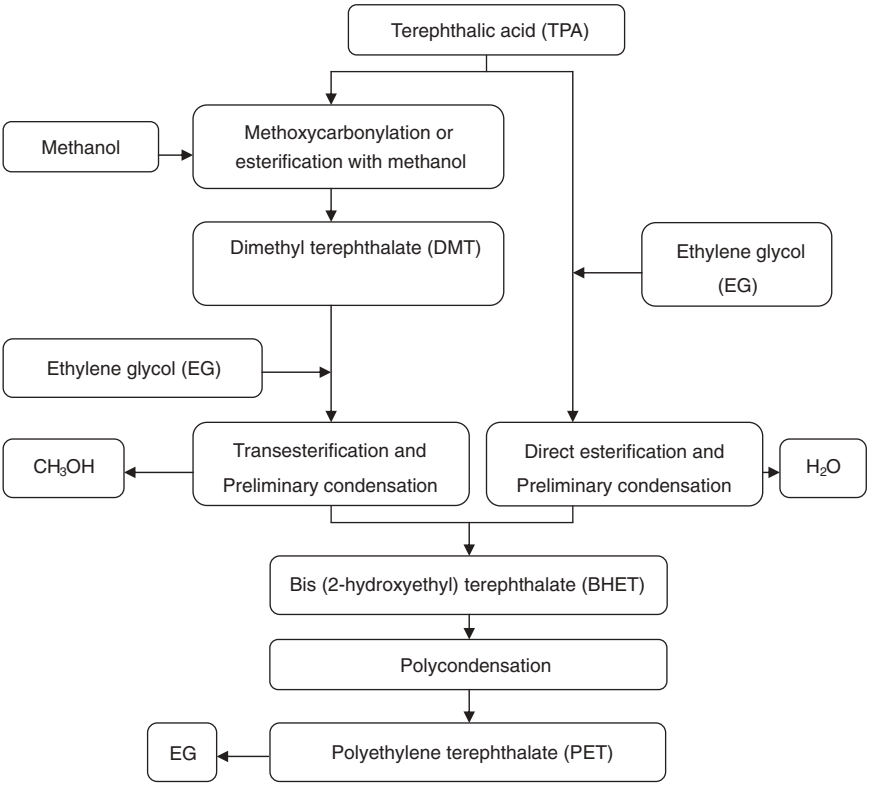

3.3 Flow chart of PET process.

Currently, the one-step oxidation of *p*-xylene is commonly adopted. Terephthalic acid and dimethyl terephthalate are purified and then used as raw materials for polyester fibre production.

3.3 Polymerisation process of polyester fibres in industry

In industrial practice, the polymerisation processes of aromatic polyethylene terephthalate are produced via a two-step process. The first step is esterification and preliminary condensation, while the second is polycondensation or melt polymerization.[15] The flow chart for polyethylene terephthalate (PET) process is depicted in Fig. 3.3.

3.3.1 Esterification and preliminary condensation

Esterification and preliminary condensation proceed in two paths: (1) transesterification and preliminary condensation and (2) direct esterifica-

tion and preliminary condensation. In the first path, the DMT is transformed, with the assistance of one or more catalysts and EG at temperatures ranging from 150 to 200°C, into BHET (bis-(2-hydroxyethyl) terephthalate) (also called diglycol terephthalate, DGT) with the elimination of methanol. The reactions of first path proceed as follows:

Transesterification

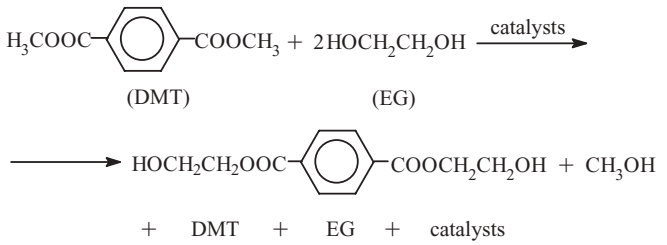

Preliminary condensation

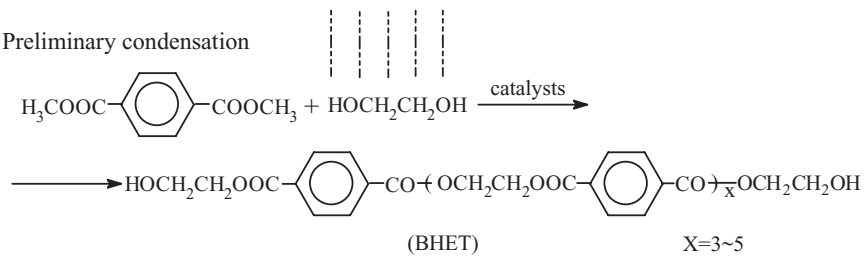

The reaction conditions of transesterification and preliminary condensation are:[16]

- Catalysts: metal oxides (PbO, MgO, Sb_2O_3, etc.), metal acetates (Co, Mn, Zn, etc.), or mixtures of oxides and acetates metals $(CH_3COO)_2CO$-Sb_2O_3, $(CH_3COO)_2CO$-PbO, etc.).
- Concentration of catalyst: 0.05% (to the amount of DMT).
- Monomer ingredient for DMT: EG = 1: (2~2.5) (mole ratio).
- Reaction temperature: falls in the range of 150–200°C (gradually increases).
- Reaction time: 3–6 hours.

In the second path (direct esterification and preliminary condensation), terephthalic acid (TPA) is converted, with EG and the aid of one or more catalysts at temperatures ranging from 250 to 280°C, into BHET with the elimination of water. The reaction is explained in the following scheme:

Direct esterification

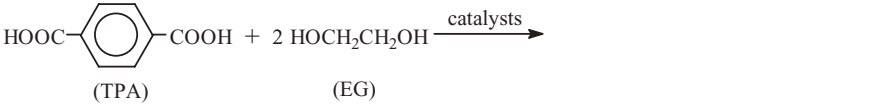

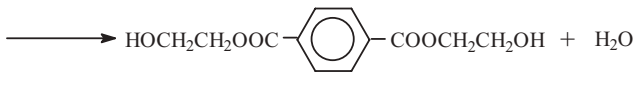

+ TPA + EG + catalyate

Preliminary condensation

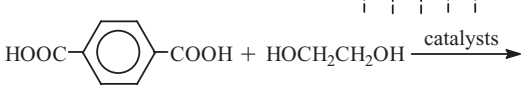

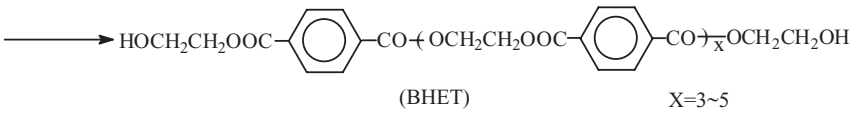

The reaction conditions of direct esterification and preliminary condensation are:

- Catalysts: metal oxides (Sb_2O_3, PbO, etc.).
- The concentration of catalysts: should be less than 0.05% (to the amount of TPA).
- Monomer ingredient for TPA: EG = 1: (1.1–2) (mole ratio).
- Reaction temperature: 250–290°C (increases gradually).
- Reaction time: 3–6 hours.

3.3.2 Polycondensation

This step starts by the BHET produced by esterification and preliminary condensation. Then, by condensation reaction, the intermolecular BHET releases EG and produces PET. The reaction is:

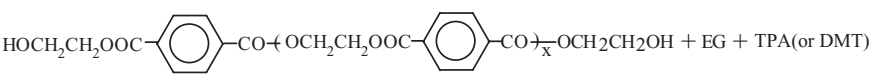

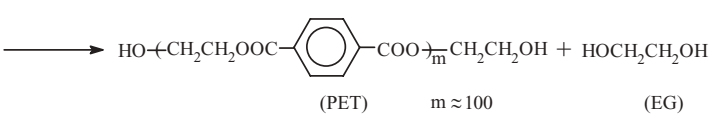

The reaction conditions of polycondensation are:[5]

- Catalysts: metal acetates (e.g., Co, Mn, Zn, Mg, Pb, Cd, etc.) or mixtures of oxides and acetate metals; such as $(CH_3COO)_2Mn + Sb_2O_3$, $(CH_3COO)_2Co + Sb_2O_3$, etc.
- The concentration of catalysts: 0.02–0.03% (to the amount of TPA or DMT).
- The thermal stabilizer of PET: phosphor compounds.
- The concentration of the thermal stabilizer of PET: 0.015–0.03% (to the amount of TPA or DMT).
- Nitrogen under pressure is needed to place BHET into the condensation vessel.
- Reaction temperature: 265–285°C (stable temperature).
- Reaction pressure: below 1 mm/Hg.
- Reaction time: 4–6 hours.

3.4 Fundamental principles and types of melt spinning process

The spinning process of fibre-forming polyester converted to fibre passes into three stages. In the first stage, a solid fibre-forming polyester is produced from polymerisation, which is called polymer chips. Polyester chips are converted to dope by heat, or by dissolving in some solvent.

$$\text{Polymer chips} \xrightarrow{\text{Conversion}} \text{Dope (viscoelastic fluid, or spinning fluid)}$$

In the second stage, dope fluid is extruded through a spinneret and then converted to viscoelastic filament (also known as the originally extruded filament). The viscoelastic filament is solidified into solid filament fibre (usually called filament), which may be formed by extending the viscoelastic filament.

$$\text{Dope} \xrightarrow{\text{Spinning}} \text{Viscoelastic filament} \xrightarrow{\text{Solidification}} \text{Solid filament fibre}$$

Solidification may be obtained by cooling,[17,18] by extruding the viscoelastic filament submerged in a coagulation bath for removal of the solvent,[19] or by extrusion into the heating chamber for evaporation of the solvent.[20] From both stages, there are three methods of the spinning process:

1. Melt spinning:

$$\text{Polymer chips} \xrightarrow{\text{Conversion by heat}} \text{Dope} \xrightarrow{\text{Spinning}} \text{Viscoelastic filament} \xrightarrow{\text{Solidification by cooling}} \text{Solid filament fibre}$$

2. Wet spinning:

$$\text{Polymer chips} \xrightarrow{\text{Conversion by dissolving in solvent}} \text{Dope} \xrightarrow{\text{Spinning}} \text{Viscoelastic filament} \xrightarrow{\text{Solidification by submerging in coagulation bath}} \text{Solid filament fibre}$$

3. Dry spinning[21,22]:

$$\text{Polymer chips} \xrightarrow{\text{Conversion by dissolving in solvent}} \text{Dope} \xrightarrow{\text{Spinning}} \text{Viscoelastic filament} \xrightarrow{\text{Solidification by curing in the heating chamber}} \text{Solid filament fibre}$$

If the polymer chips are thermoplastic polymers (i.e., PET, polyamide, polyurethane, polypropylene, etc.), melt spinning, wet spinning or dry spinning can be used. Usually, melt spinning is used. But if polymer chips are thermosetting polymers (i.e., polyacrylonitrile, viscose rayon, cellulose acetate, etc.), wet spinning or dry spinning can be used.

In the third stage, when the viscoelastic filament is solidified into solid filament fibre, it is extended by the drawing process. The drawing process decreases the diameter, and the orientation of solid filament fibre could increase, while it improves the degree of crystallinity.

3.4.1 Fundamental principles of melt spinning process

PET belongs to the thermoplastic polymer and so the commercial PET fibre usually uses melt spinning. The schematic melt spinning process for PET fibre is shown in Fig. 3.4.[23] PET fibres are formed by extrusion of the molten polymer. Apparently, this is a simple process. A supply of molten PET (D) is pumped at a constant rate and under very high pressure through small holes in the spinning jet (E). The viscoelastic filaments are extruded to emerge vertically downwards from the face of the spinning jet and, on cooling (F), solidify, and wind onto the bobbins.

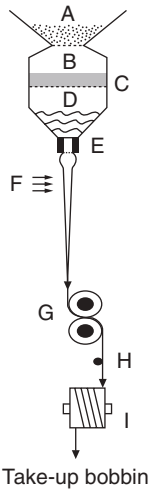

A. Hopper fed with PET chips
B. Spinning vessel
C. Heated grid
D. Dope (molten PET)
E. Spinning jet (spinneret)
F. Cold air
G. Input feed rollers
H. Deflector
I. Output feed roller

3.4 Schematic melt spinning process for PET fibre.

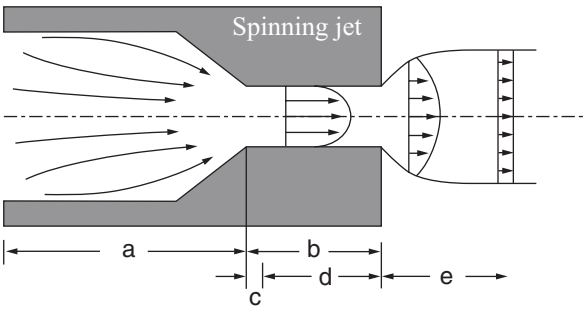

a. Fluid guide hole
b. Spinneret hole tube
c. Fluid inlet zone
d. Fluid entire extended zone
e. Fluid jet issuing zone

3.5 The profile model of spinning jet.

In Fig. 3.4, the profile model of dope fluid (viscoelastic fluid) flows through the spinning jet (E), which is described in Fig. 3.5.

In the inlet zone (c), the dope fluid is contracted, and then the polymer chain in the dope fluid produces elastic deformation. In the entire extended zone (d), the velocity of viscoelastic fluid is a steady flow. The contraction phenomenon of viscoelastic fluid in the jet issuing zone (e) is related to the different velocity profiles inside and outside the spinneret hole tube. The fluid jet expands outside the spinneret hole tube and its maximum radius is often called die swell.[17] The profile of total energy transformation of the dope fluid flowing through spinneret hole tube is illustrated in Fig. 3.6.

Dope fluid (viscoelastic fluid) is extruded through the spinneret, and then converted to viscoelastic filament. The viscoelastic filament is transformed into solid filament fibres by cooling, where the viscoelastic filament

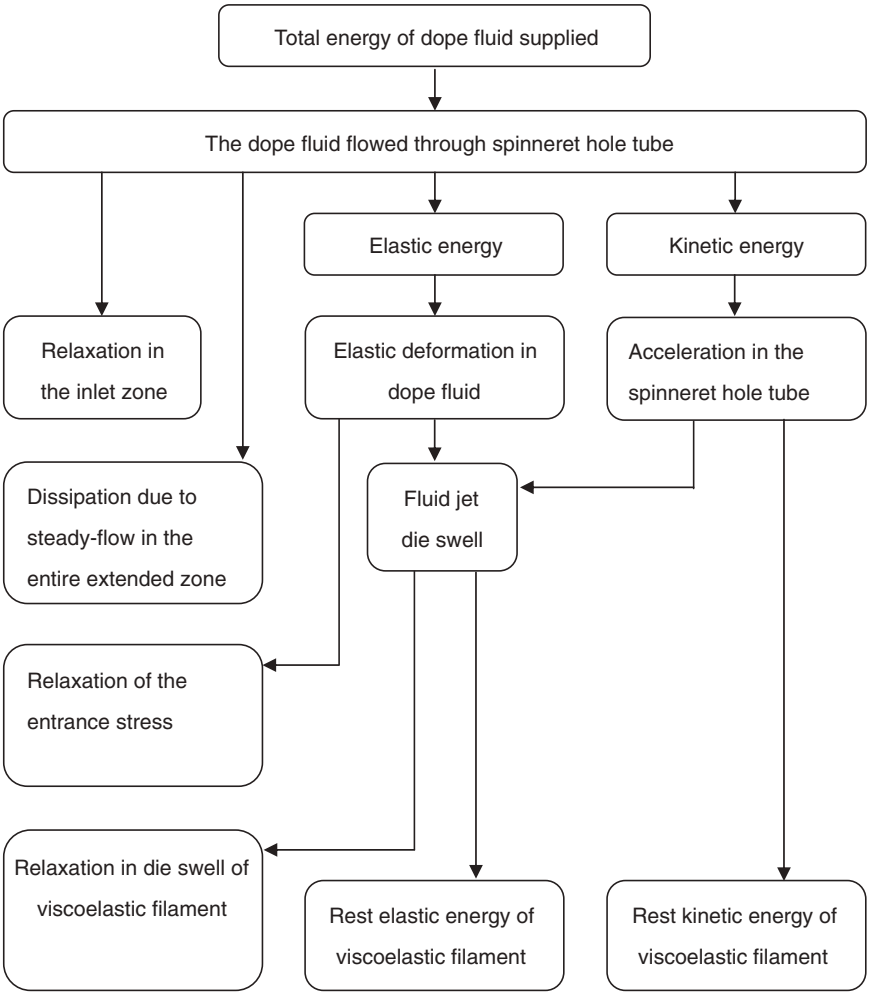

3.6 The profile of total energy in spinneret dope fluid.

will be extended and the diameter of the viscoelastic filament will be reduced. The entire deformation process of the viscoelastic filament by elongation strain can be divided into three sections as shown in Fig. 3.7:

(a) Die swell section with negative parallel (elongation) velocity gradient.
(b) Elongation section (or deformation section) with positive parallel (elongation) velocity gradient.
(c) Solid motion section (running solid filament fibre section) with zero parallel (elongation) velocity gradient or without deformation.

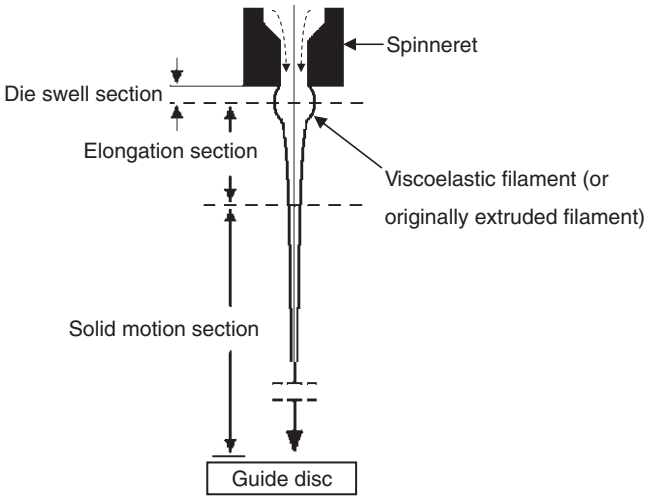

3.7 The deformation of viscoelastic filament (dope filament) by elongation strain.

The diameter of the viscoelastic filament is maximum at the intersection of the die swell and elongation sections. The distance is usually less than 10 mm from the spinneret. The distance of the elongation section is usually 50–150 cm from the spinneret. The viscoelastic filament (originally extruded filament) on the spinning axial line is then solidified by cooling. During solidification there are two temperature gradients. The first temperature gradient is along the spinning axial line, while the other is radial which expresses the radial differential temperature from the outer layers to the inner layers of viscoelastic filament. Although the range is only a few degrees celsius, the physical properties of viscoelastic filament may be significantly affected. Fig. 3.8 displays the influence of physical properties on the viscoelastic filament.[24]

The following results are obtained from Fig. 3.8 regarding:

(a) Temperature: the outer layers are lower, while the inner layers are higher.
(b) Crystallisation rate: the outer layers are fast, while the inner layers are slow.
(c) Viscosity: the outer layers are high; however, the inner layers are low.
(d) Axial spinning velocity: uniform velocity on radial.
(e) Extensional force: the outer layers are high, whereas the inner layers are low.

Drawing of PET viscoelastic filaments or filament (solid filament fibres) may be performed, depending on the fibre type, under cold or hot

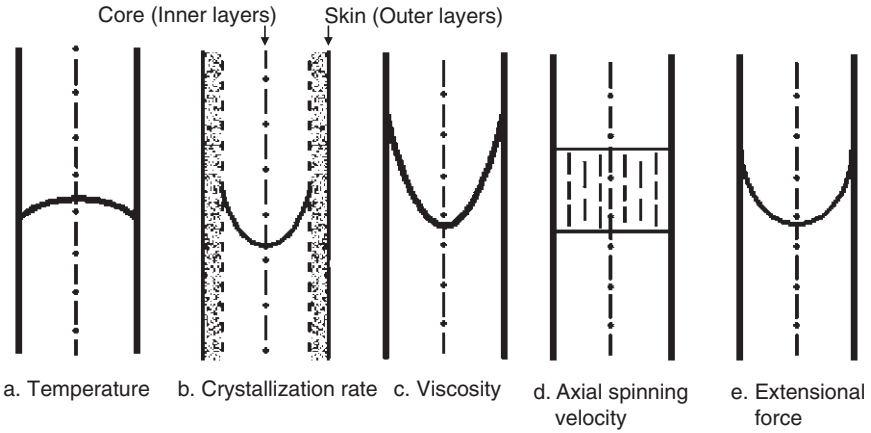

3.8 The influence of physical properties on viscoelastic filament.

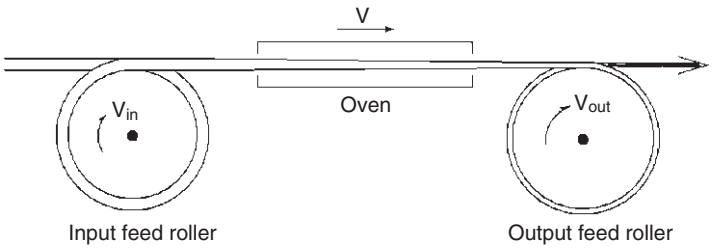

3.9 Scheme of the continuous drawing process.

conditions, besides it has an additional effect of making the filament both narrower and longer. The drawing process is usually performed at a temperature that must be higher than the secondary transition temperature (T_g) of PET fibres. The drawing process is achieved by stretching the viscoelastic filament between two rollers (input feed roller and output feed roller), called godet rolls, with the output feed roller rotating faster. It also may be performed immediately after spinning of viscoelastic filament or during subsequent processing as part of yarn texturing and/or spinning.

The industrial drawing depicted in Fig. 3.9 is a continuous operation. In this process, the PET filament is supplied at the input feed roller with a constant feed velocity, V_{in}, and is taken-up by the output feed roller running with a constant drawing velocity, V_{out}, equalling $R \times V_{in}$; where R is the nominal draw ratio. The actual draw ratio is less than R because the drawing filament shrinks when tension is removed.

The stress-strain curve (S-S curve) of the PET viscoelastic filament during the drawing process is shown in Fig. 3.10. From this figure, it is

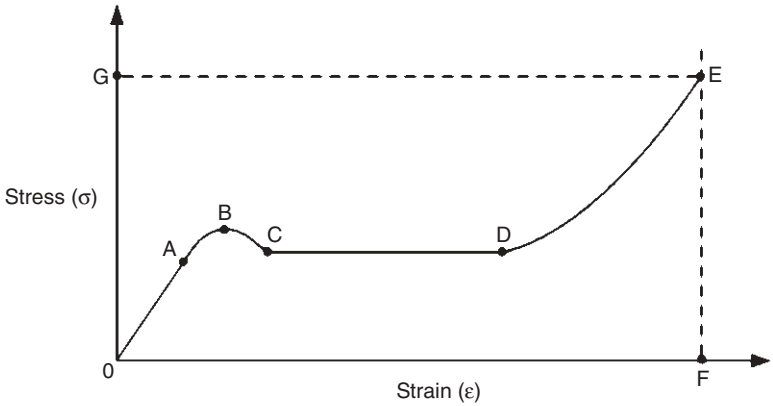

3.10 Fundamental of PET viscoelastic filament deformation characteristics.

noted that the deformation in the *OA* region is uniform and is usually reversible. The slope of S-S curve (called modulus = σ/ε) is constant. The deformation is called elastic deformation. In the *AB* region, the modulus decreases when the stress is increased. The drawing exhibits a non-uniform deformation. The largest stress corresponds to point *B* which is often called the yield point. In the *BC* region, the deformation is unstable, where local attenuation results in a 'necking effect' concentration of stress. The strain is called strain-softening. The *CD* region is called the necking effect region. The deformation is concentrated in one or more necks, which gradually extends over the entire filament, while the diameter of the neck and undrawn parts remains steady. The deformation in this region is irreversible. In the *DE* region, the deformation is uniform and is usually irreversible. The strain increases as the stress increases. The drawing exhibits a uniform deformation. Point E is called the breaking point. Finally, the *OF* and *OG* are called the breaking strain and the breaking stress, respectively.

Crystalline and amorphous arrangements of PET chain exist within newly formed filaments. These PET chain molecules are possibly oriented to make them more parallel to the walls of the filament by stretching the filament before it is completely solidified. This results in more crystalline and stronger filaments. However, not all filaments are drawn to the maximum amount possible, because when a filament fibre reaches its maximum length, the extensibility of filament fibres (or filament yarn) decreases.[25] Therefore, filament yarn can be divided into two types based on the degree of drawing (called the draw ratio). The filaments that have not been fully drawn are called partially oriented yarns (POY), while those that have been fully drawn are called fully oriented yarns (FOY).

3.4.2 Fundamental types of melt spinning processes

There are two procedures for the production process of PET fibre. The first procedure is the production process for PET, while the second one is the melt spinning process for PET fibres.

Production processes for polyethylene terephthalate

There are two production processes for producing PET including batch process and continuous process. These two processes are illustrated as follows:

1. Batch process, which proceeds as follows:

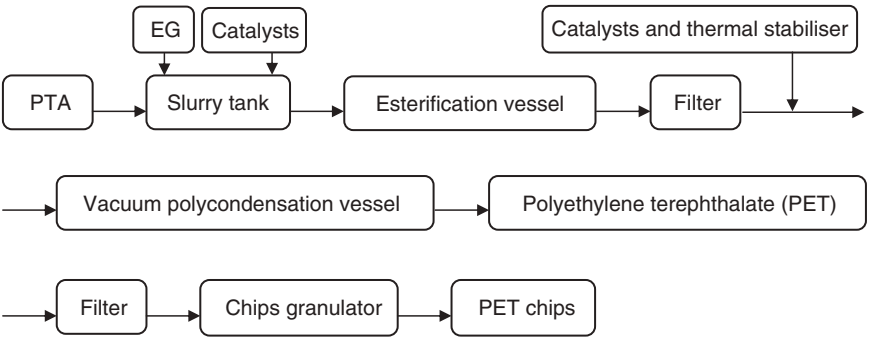

2. Continuous process, which is conducted as shown below:

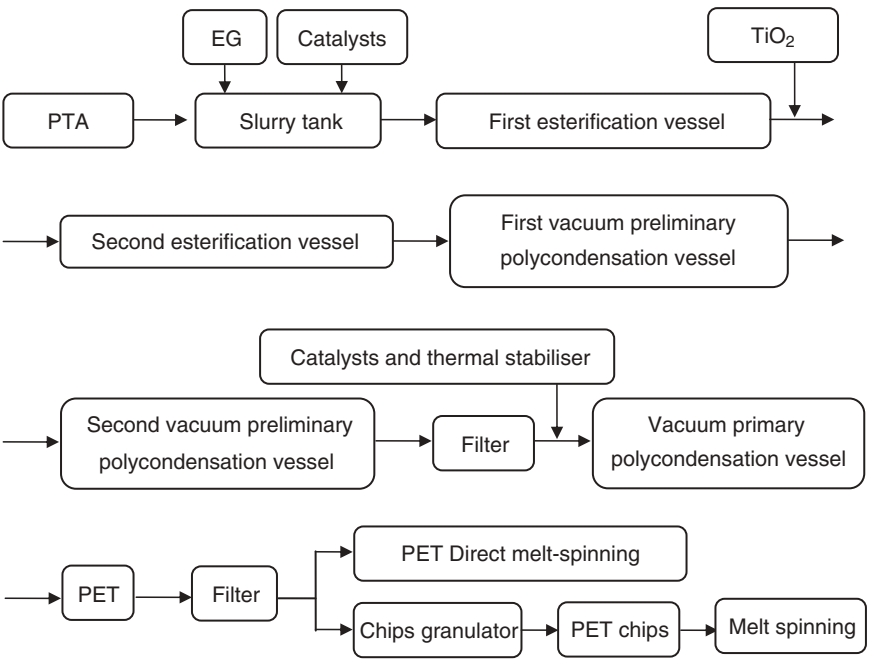

Melt spinning process for polyethylene terephthalate fibres

PET staple fibres and PET filament fibres are produced by melt spinning processes as follows:

1. PET staple fibres production

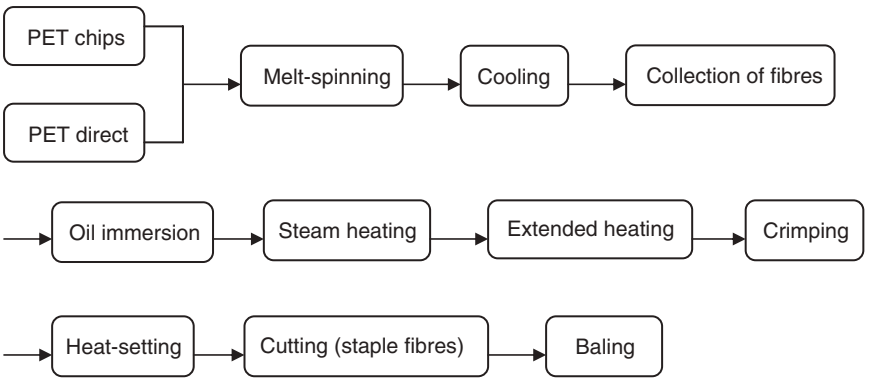

2. PET filament fibres production

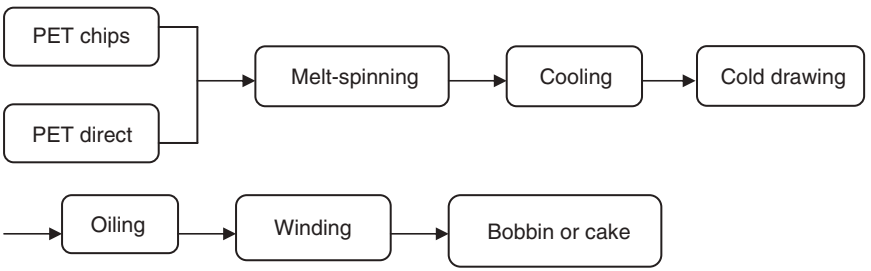

3.5 Heat setting and textured yarn of filament

3.5.1 Heat setting

In the melt spinning process, the time of fibre-forming is usually short. This results in different relaxing states of polymer chain in the PET fibre and causes non-uniform internal stresses within it. In effect, many crystal defects appear. Moreover, such an unstable structure would cause fibre shrinkage that makes any further finishing processes so difficult. Thus, in order to achieve a stable fibre structure, heat setting should be controlled before the fibres are used.

Heat setting determines the morphology and dimensional stability of thermoplastic fibres. It includes three fundamental factors: temperature,

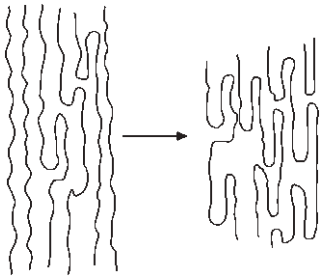

(a) Before heat setting (b) After heat setting

3.11 Effect of heat setting on fibre structure.

time and speed. In practice, temperature should be set greater than the secondary transition temperature (T_g) and below the melting temperature (T_m). Heat setting causes the movement of polymer chains in fibres, which releases the internal stress, finally producing a complete and stable structure of fibres as shown in Fig. 3.11. Dismore and Statton[26] show that the polymer chain would change into a fold when the heat setting temperature is increased.

The heat-setting process passes through three stages. The first stage is called the fibre structure loosing stage in which, due to heating, the fibre temperature is higher than T_g. However, the interaction force between the PET chain in fibres is weakened in a few seconds. The second stage is an actual heat-setting stage in which the binding energy between the PET chain spontaneously increases, while the PET chain produces heat-vibration. Because of the fibre structure loosing stage and the heat-vibration phenomenon, a new binding force between PET chains (in fibre) is formed. The completion time of this stage is several times that of the first stage. Finally, in the third stage, the binding force and the structure of the PET chain are fixed when the fibre temperature is kept below T_g. In practice, this stage can be completed in a few seconds.

3.5.2 False-twist process

In 1954, the first machine for false-twist was invented. This machine can produce a filament yarn with stretchability. The fundamental principle of the false-twist process is to change the straight multi-filaments into a crimp filament. In this process, the straight multi-filament is placed at a system above T_g. Then, it is twisted with force to re-arrange the internal molecule and form a perpetual deformation. The main characteristic of the false-twist process is to rotate the middle of the multi-filament so that the twist numbers at both sides of the rotation point are equal in each direction[27] as shown in Fig. 3.12(a).

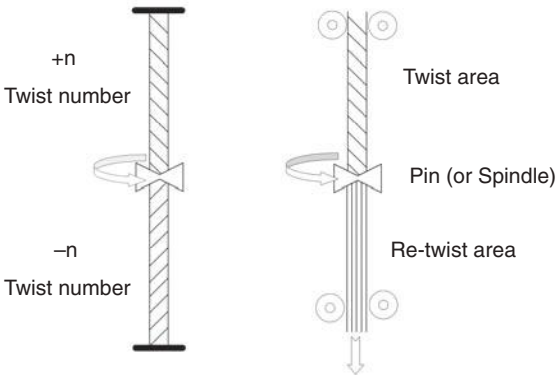

(a) Twist number setting (b) False-twist process

3.12 Illustration of false-twist.

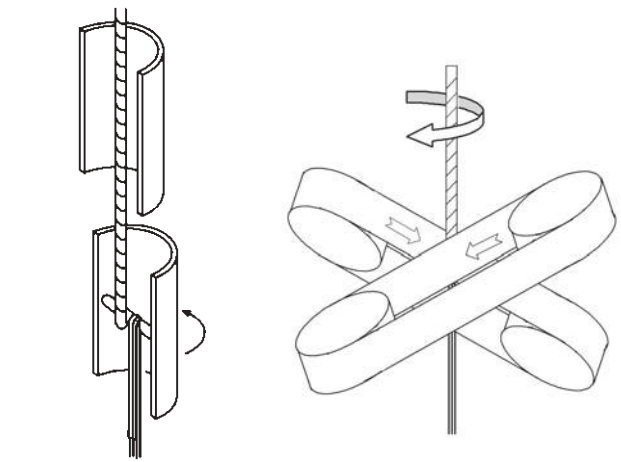

(a) Pin-type spindle twisting (b) Friction twisting

3.13 The mechanism of false-twist types.

The false-twist process shown in Fig. 3.12(b) sets a heater in the twist area while the crimp of the filament is fixed. When the multi-filament is twisted through the pin (or spindle) into the re-twist area, the twist number of the multi-filament becomes zero while each monofilament holds the crimp shape.

The false-twist process includes twist, heat setting and re-twists. Generally, textured yarn is produced by the false-twist process. Two types of false-twist process exist. The first is pin-type spindle twisting, while the other is friction twisting. The mechanisms of these two types are illustrated in Fig. 3.13.[28]

3.6 High speed spinning and novel spinning

3.6.1 High speed spinning of polyester filaments

The first concept of high speed spinning was developed by DuPont's US patent in 1952.[29] Along with the development of industrial technology, the high speed take-up machine for above 6000 m/min was developed in 1980. High speed spinning was then commercialized. Due to the continuous development of mechanism and electronic control systems, it is expected that the spinning speed will reach 8000 m/min during the twenty-first century. Meanwhile the spinning speed for research in the laboratory is over 12 000 m/min.

Fundamental principles of high speed spinning

High speed spinning was developed based on the conventional spinning method of 1500~2500 m/min speed. This process combines the spinning and drawing processes, which are performed at a speed ranging between 3500~4000 m/min, in the same machine. The take-up of the fibre takes place with a winding speed of 5000~6500 m/min.[30]

The key point of high speed spinning is the orientation of molecules, which is influenced by several spinning parameters; especially spinning tension. Spinning tension is related to the spinning speed, the raw material property, and the processing conditions; including process temperature, the condition of quenching, and the spin-draw ratio of spinneret.

The polymer melt deformation in the high speed spinning process is shown in Fig. 3.14. It is noted that the fibre forming structure is divided into three zones: (I) flow-deformation, (II) oriented-crystallisation, and (III) plastic-deformation. When the polymer melt passes through the spinning jet and emerges from the spin holes into the air, it is normally solidified in a distance of 30–130 cm from the surface of spinneret (depends on the spinning condition). Therefore, the structure of the fibre will be changed. The basic parameters of fibre structure are birefringence, crystallisation, and crystal size. Normally, birefringence and crystallisation of partially oriented yarn are increased by raising the spinning speed of the fibre. In effect, tenacity is increased, while the elongation of the fibre is reduced.

High speed spinning process

Manufacturers prefer a process that produces a full oriented yarn with one single machine. Therefore, the high speed spinning process was developed in various methods.[31,32]

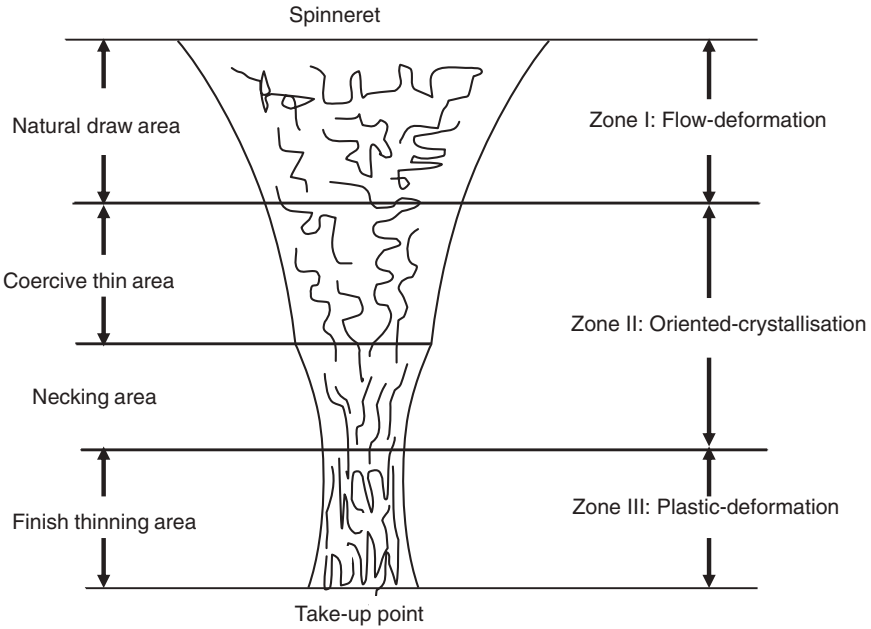

3.14 The forming structure of PET high speed spinning.

It is well known that the basic process of melt spinning includes: the melting condition of polymer, the through-put of melt from the spinneret, the thinning process of the polymer melt (viscoelastic filament), the solidification of the viscoelastic filament, and the oil pick-up and fibre take-up procedure.

The high speed spinning process is improved from the conventional melt spinning technology by increasing the spinning speed to 3500 m/min, adding the drawing rollers to three or more heated godets, and raising up the winding speed to 5000–6500 m/min. High speed spinning process is depicted in Fig. 3.15.

In Fig. 3.15, the yarn path goes through rollers 1 and 2, where the speed of roller 2 is greater than 3500 m/min. The drawing process is then performed with different operation speeds of rollers 2 and 3, where the speed of roller 3 could be raised to 5000–6500 m/min. Finally, the yarn is taken-up by a high speed winding machine so that a full oriented yarn is obtained.[33]

When using the high speed spinning process, the production capacity may be increased by more than 20%. In return, the production cost would be reduced effectively. However, high spinning speed causes higher winding tension of yarn and, consequently, increases the instability of the spin-line.

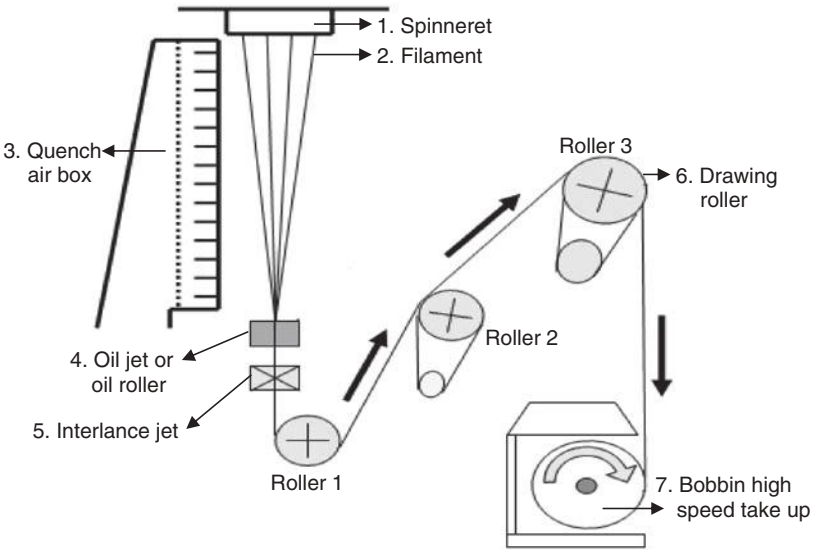

3.15 High speed spinning process.

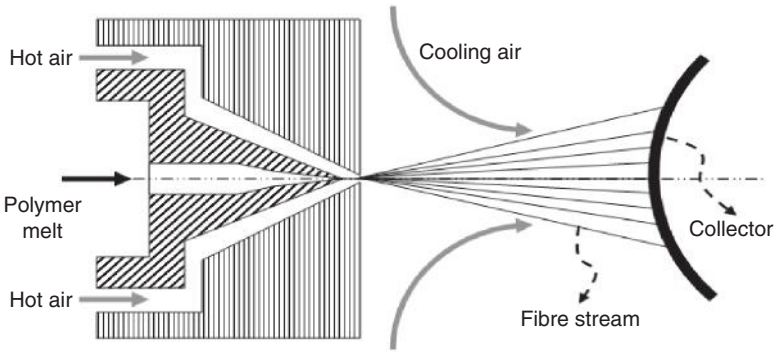

3.16 Scheme of melt blown process.

As a result, an optimal oil application and effective performance of yarn guides are critical for the success of this process.

3.6.2 Novel spinning of polyester fibres

Melt blown process

Melt blown process, shown in Fig. 3.16, was initially developed by Naval Research Lab, USA in 1951.[30] Then, it was classified as melt spun nonwoven process.[34,35] By this process, almost all the thermoplastic polymer can

be produced with micro-fibre. The diameter of single fibre from the melt blown process is 1 micron or less, but the variation of the fibre size is relatively high. The tensile properties of melt blown nonwoven for machine direction and cross direction show an obvious uneven behaviour. Since melt spinning has an advantage for mass production, researchers focus on the improvements for the melt blown process. For example, the design of a special spinning device and spin pack to reduce the fibre size to submicrons, where it is expected to achieve a nano-scale fibre with a cost below $US10; Nanoval Co. from Germany was authorised by Neumag Co. to develop an air impingement method to make ultra-fine fibres; and Hills Co. of USA design the thin distribution plates to enlarge the spin holes per unit area of spin pack and thus the through-put per hole will be reduced and consequently a finer fibre can be attained.[36] In addition, the alternation of L/D for spin hole may help in reducing the melt blown fibre dimension. The ideal diameter of the spin hole is around 0.10–0.15 mm, while the optimum melt flow index of the polymer is controlled at 1000.

Split conjugate spinning process

It is very hard to produce a micro-fibre with the denier per filament below 0.3 denier by a conventional single component method.[37,38] Before 1960, there was no commercialised technology for micro-fibre. In 1970, Toray Co. in Japan started its promotion of micro-fibre products. The spilt conjugated bi-component fibre is an approach for producing micro-fibres, which includes two incompatible polymers such as PET and PA6, using the conjugate spinning method[39,40] to spin to fibre. These two polymers are distributed similarly to the petal segments type on fibre cross-section. Each conjugated filament is then divided into several finer fibres by means of a mechanical or a chemical method. It can possibly be split during the fabrication and dyeing process into 12, 16, 24 or 32 segments, and so on, depending on the design of the spin pack. This method is called the split conjugated micro-fibres. After splitting the denier of fine fibre may reach 0.03–0.07 denier. The end product using this micro-fibre is suitable for several products including high quality wipers and high density fabrics for apparel and home textiles. Figs. 3.17 and 3.18 display the schemes of split conjugate fibre for (24 segment-pie) and spin pack for split conjugate fibre, respectively.

The purpose of split conjugated micro-fibre is to get a fine fibre by the splitting of the interface of two polymers. In this process, the appropriate design of conjugate configuration is very important and the viscosity of the independent polymer is critical. If there is a huge difference of flow behaviour between two polymers, an undesirable conjugate configuration results which may influence the splitting effect of the filament. The shape of the

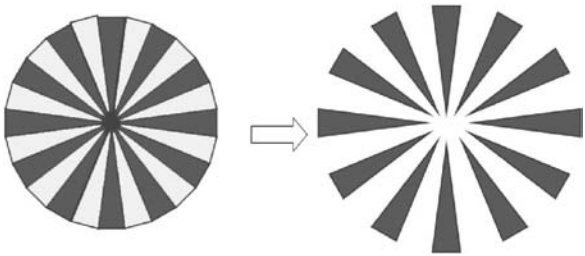

3.17 Scheme of split conjugate fibre (24 segment-pie).

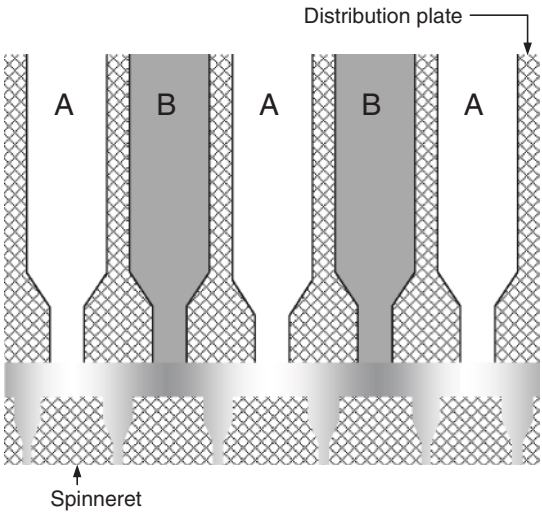

3.18 Scheme of spin pack for split conjugate fibre.

fine fibre after splitting is a geometrical triangle that makes the split micro-fibre suitable for wiping application.

Sea and island conjugate spinning process

Polymer modification technology is used to create an alkali soluble type of copolymer. Then, the copolymer is spun with a regular polymer. The resulting fibre cross-section shows multi-islands distributed in a sea component. The sea component is then removed by the alkali soluble effect during the fabrication and dyeing process. Finally, the independent island component becomes a very fine fibre as shown in Fig. 3.19. This process is called the sea and island conjugate micro-fibres.[41]

The common polymer used for sea and island conjugate fibre is polyester, the denier per fibre after alkali treatment is around 0.02–0.06 denier. If a spunbonded nonwoven process is utilized, fineness may reach 9×10^{-5}

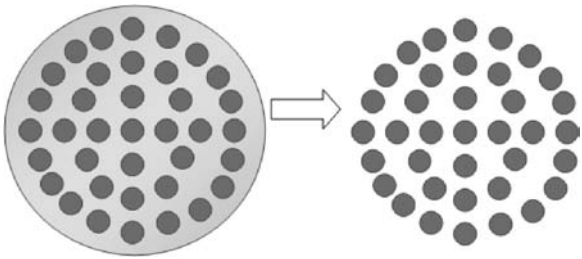

3.19 Scheme of sea and island conjugate fibre (37 islands in sea).

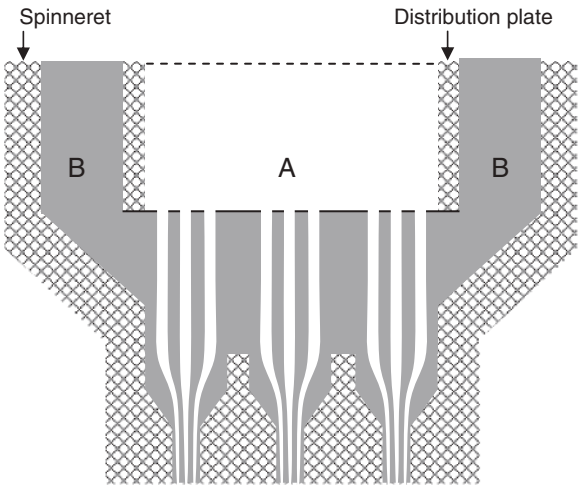

3.20 Scheme of spin pack for sea and island conjugate fibre.

denier and the diameter of fibre is 0.1 micron. The end product from sea and island micro-fibre process could be high quality artificial leather which is used for apparel and other textiles industries. Figure 3.20 displays the scheme of spin pack for sea and island conjugate fibre (37 islands in the sea).

The appropriate conjugate ratio of alkali soluble component is 15–30%, which will be removed out during dyeing process. The flowing behaviour of this easily soluble polymer should ensure that the island component will be enveloped completely to prevent the stickiness of islands from influencing the evenness of fine fibre separation. Easily soluble polyester is developed by introducing a polymer, such as polyethylene glycol (PEG) and other monomers, to reduce resistance for the alkali solution. The alkali soluble effect of easily soluble polyester may reach 100 times that of regular polyester.

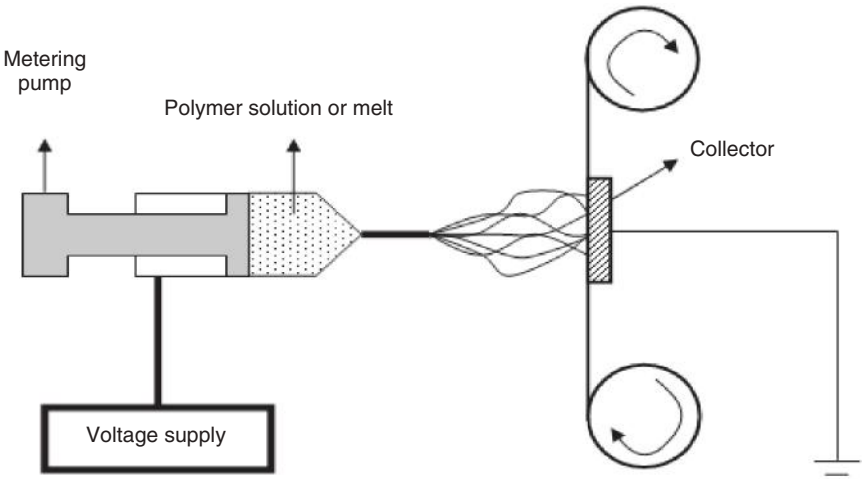

3.21 Scheme of electro-spinning device.

Electro-spinning process

Electro-spinning is the earliest method for the formation of nanoscale fibres.[42,43] The scheme of the electro-spinning device is shown in Fig. 3.21. Polymer solution or melt is delivered by a capillary injection tube. A 30~50 kV high voltage is supplied by a power unit so that the polymer is dragged by the electric charge forming the fibre profile. Fibre from the electro-spinning process is non-oriented, so that it is hard to produce continuous filament. Thus, the fibre is formed as a nonwoven structure with diameter of fibres around 10^0–10^1 nm. The tenacity of electro-spinning fibre is relatively low, which affects its application possibility.

The most significant property of polymer used for electro-spinning is viscosity and electron conductivity. The former is related to spinnability, while the latter is related to the extent of polymer dragged by the electric charge. The characteristic of electro-spinning is ease of operation for manufacturing micro-fibres with a high specific surface area of textile structure. The end product is good for industrial filtration. In addition, electro-spinning technology may have the potential for the development of tissue engineering material and artificial blood vessels for biomedical applications.

3.7 Acknowledgements

I would like to thank Dr Kuen-Shan Hwang from Acelon Chemicals and Fiber Corporation in Taiwan, Ta-Chung An from Taiwan Textile Research

Institute, Chun Lin at the Department of Materials Science and Engineering, and Abbas Al-Refaie at the Department of Industrial Engineering and Systems Management in Feng Chia University, Taiwan, for their support.

3.8 References

1. PETERS R H (1968), *Textile Chemistry*: *The Chemistry of Fibres*, Vol. 1, New York, Elsevier.
2. MARK H and WHITBY G S (1940), *Collected Papers of Wallace Hume Carothers on Polymerisation*, New York, Interscience Publishers Inc.
3. CAROTHERS W H and ARVIN J A (1929), *J. Am. Chem. Soc.*, 51, 2560.
4. SPANAGEL E W and CAROTHERS W H (1935), 'Macrocyclic esters' *J. Am. Chem. Soc.*, 57, 929–34.
5. HERMANN L (1971), *Polyester Fibres: Chemistry and Technology*, New York, Wiley-Interscience.
6. CAROTHERS W H and HILL J W (1932), *J. Am. Chem. Soc.*, 54, 1579.
7. LUDEWIG H and RAMM H (1956), DWP 14 854.
8. POHL H A (1951), 'The thermal degradation of polyesters', *J. Am. Chem. Soc.*, 73, 5560–1.
9. MCMAHON W, BIRDSALL H A, JOHNSON G R, and CAMILLI C T (1959), 'Physical properties evaluation of compounds and materials', *Journal of Chemical and Engineering Data*, 4, 57–79.
10. Chem. Fabr. Kalk.: D. R. P. 416 604.
11. RaeckeB: D.B.P. 958 920 (patent).
12. Chem. Werke imhausen, E.P. 787 054 (Patent).
13. D A S (1953), 1 028 983 (Patent).
14. BARRET K E and MARKS A: E.P. 735 074 (Patent).
15. MARK H *et al.* (1988), *Encyclopedia of Polymer Science and Engineering, Vol. 12*, New York, John Wiley & Sons, Inc.
16. WHINFIELD J R (1946), *Nature*, 158 930 (Patent).
17. ANDRZEJ Z (1967), *Physical Fundamentals of the Fiber-Spinning Processes, and Principles of Melt-Spinning, in Man-Made Fibers Science and Technology, Vol. I*, New York, Wiley-Interscience.
18. THE SOCIETY OF FIBER SCIENCE AND TECHNOLOGY (1969), *Formation of Fibers and Development of their Structure*: (I) *Melt Spinning*, Japan, Kagaku-dojin, Kyoto.
19. ANDRZEJ Z (1976), *Fundamentals of Fibre Formation: The Science of Fibre Spinning and Drawing*, London, Wiley-Interscience.
20. THE SOCIETY OF FIBER SCIENCE AND TECHNOLOGY (1970), *Formation of Fibers and Development of their Structure:* (II) *Wet Spinning and Dry Spinning*, Japan, Kagaku-dojin, Kyoto.
21. FOK S Y and GRISKEY R G (1967), 'Mass transfer during spinning of fibers', *J. Appl. Polymer Sci.*, 11, 2417.
22. OHZAWA Y, NAGANO Y, and MATSUO T (1969), 'Studies and dry spinning. I. Fundamental equations', *J. Appl. Polymer Sci.*, 13, 257.
23. HILL R (1953), *Fibres from Synthetic Polymers*, Amsterdam, Elsevier.
24. KATAYAMA K, AMANO T and NAKAMURA K, KOLLOID Z (1968), 'Structural formation during melt spinning', *Colloid & Polymer Science*, 226, 125–34.

25. PHYLLIS G T and BILLIE J C (1997), *Understanding Textiles*, 15th Edition, Upper Saddle River, NJ, Prentice Hall.
26. PADEN F D and STATTON W O (2003), 'Chain folding in oriented 66-nylon fibers', *Journal of Polymer Science Part B: Polymer Letters*, 2(12), 1113–16.
27. KLEIN W (1993), *New Spinning Systems*, Cambridge, Woodhead Publishing.
28. WILKINSON G D (1967), *Textured Yarn Technology*, Decatur, AL, Monsanto Company, p. 63.
29. HEBELER H H (1952), *Yarn Process*, U. S. Patent: 2,604, 667, 1952.
30. NAKAJIMA T and MCLNTYRE J E (1994), *Advanced Fibre Spinning Technology*, Cambridge, Woodhead Publishing.
31. MONSANTO TEXTILES CO. (1974), *Draw-Textured Yarn Technology*, Decatur, AL, Monsanto.
32. SHIRLEY INSTITUTE (1976), *Developments in Texturing*, Manchester, Shirley Institute.
33. SHIRLEY INSTITUTE (1980), *Yarn texturing in the 1980s*.
34. HARRISON P W (1983), 'Developments in Non-woven Fabrics', Manchester, The Textile Institute, 66–7.
35. TOROBIN L and FINDLOW R (2001), 'Method and apparatus for producing high efficiency fibrous media incorporating discontinous sub-micron diameter fibers and web media formed thereby', US Patent 6, 183, 670.
36. JOHN H (2004), 'Production of polymeric nanofibers', *International Fiber Journal*, 48–50.
37. OKAMOTO M (1976), 'On ultra fine fibers', *Sen-I Gakkaishi*, 32, 318.
38. OKAMOTO M (1977), 'Ultra-fine fiber and its application', *JTN*, November, 94.
39. TEREZIE Z (1998), 'Introduction to bicomponent fibers', *International Fiber Journal*, 13(3), 20–24.
40. BENDER K and STIBAL W (1999), 'Bicomponent fibers – not only a product for market niches', *Chemical Fibers International*, 49, 402–5.
41. CHIN-AN L, CHUN-CHI C, and TA-CHUNG A (2006), 'Effect of blend ratio and draw ratio on the mechanical properties of PET/PP blended conjugate fibers', *Polymer-Plastics Technology and Engineering*, 45, 1339–45.
42. OMITRY M L (2003), 'Quality control in manufacturing of electrospun nanofiber composites', *International Nonwoven Journal*, 12(4).
43. LIONEL C K, GEORGE B K, FRANCES M P, and JENNIFER P (2001), 'Modeling, materials testing, nanostructures', *MPC Industry Collegiums Report*, 17(3), 1–4.

4

Manufacture of polyamide fibres

ASHWINI KUMAR AGRAWAL and
MANJEET JASSAL, Indian Institute
of Technology, New Delhi, India

4.1 Introduction

Polyamides are macromolecules which contain recurring amide groups as integral parts of the polymer backbone. And nylons are polyamides with structural units derived predominantly from aliphatic monomers. Although many reactions are known that are suitable for polyamide formation, commercially important nylons have been obtained by either of two basic approaches (polycondensation and ring opening polymerization) as represented by the following general equations:

$$\begin{aligned} &H_2N\text{–}(CH_2)_x\text{–}NH_2 + HOOC\text{–}(CH_2)_{y-2}\text{–}COOH \rightarrow \\ &\text{–}(HN\text{–}(CH_2)_x\text{–}NHCO\text{–}(CH_2)_{y-2}\text{–}CO\text{–}) + H_2O \end{aligned} \quad [4.1]$$

Equation (4.1) refers to the synthesis of AABB-type nylons through polycondensation of bifunctional monomers utilizing stoichiometric pairs of dicarboxylic acids and diamines,

$$H_2N\text{–}(CH_2)_{z\text{-}1}\text{–}\ COOH \ \rightarrow \ (\text{–}HN\text{–}(CH_2)_{z-1}\text{–}CO\text{–}) + H_2O \quad [4.2]$$

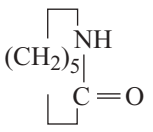

$$\rightarrow \ (\text{–}HN\text{–}(CH_2)_{z-1}\text{–}CO\text{–}) \quad [4.3]$$

Equations (4.2) and (4.3) pertain to the synthesis of AB-type nylons entailing respectively the polycondensation of aminoacids and the ring-opening polymerization of lactams.

The polycondensation Reactions (4.2) and (4.3) proceed by a mechanism that is characterized by what is generally known as carbonyl addition-elimination reactions which may be catalyzed or uncatalyzed.

Assuming equivalence of all the amide groups formed and independence of the functional groups from the molecular chain length, the polymerization reaches equilibrium. This may be represented by the equation

$$-NH_2 + HOOC- \Leftrightarrow -NHCO- + H_2O \quad [4.4]$$

The equilibrium constant K for the above reaction is defined as:

$$K = \frac{[NHCO][H_2O]}{[COOH][NH_2]} \quad [4.5]$$

where B is the temperature independent part of equilibrium constant and ΔH_a is the enthalpy change of the polymerization reaction. The reaction is exothermic and the ΔH_a values in the range of –25 to –29 kJ mol^{-1} are reported.[1,2] Therefore, a decrease in temperature favors a polymer of higher molecular weight if water concentration is constant. The molecular weight of the resulting polyamides will, thus, always remain finite and be affected considerably by any stoichiometric imbalance of the end-groups. Non-equivalence of the concentration of the bifunctional reactants and addition of monofunctional species (such as acetic acid) are practiced for molecular weight control, also known as stabilizers.

Two commercially important textile grade fibres belonging to this chemical class are nylon 6 (AB type) and nylon 6,6 (AABB type). The design of an optimal process and reactor system is possible only when it is based upon a thorough understanding of the mechanism and kinetics of the polymerization process. Therefore, a considerable amount of research has been directed to investigate the polymerization mechanisms and to determine the kinetic and thermodynamic parameters of the polyamide-forming reactions.

4.2 Nylon 6,6

Nylon 6,6 is prepared from polycondensation of hexamethylene diamine (HMD) and adipic acid. The repeat unit of the polymer is –NH $(CH_2)_6$ NH $CO(CH_2)_4CO$–. The diamine, which melts at 40.87°C, is normally used in the form of a concentrated aqueous solution. The dibasic acid is used in its pure solid form (m.p. = 152.1°C). In the preparation of nylon 6,6 polymer, the first step is preparation of salt from precisely stoichiometric quantities of the intermediates at room temperature. The salt can be prepared by mixing the alcoholic solutions of the two components, the pure salt precipitates and is dissolved in water to give a solution. Alternatively, the salt can be prepared by mixing a dispersion of the diacid in water with a solution of the diamine. The aqueous salt solution is prepared so that it has a concentration of about 50–60%. The stoichiometric equivalence is

determined by measurement of the pH of a 9% salt solution prepared by dilution of main salt batch. The pH at equivalence is about 7.6 for this concentration and a shift of pH of only 0.1 results in a change in end group balance of about four equiv. 10^{-6} g. This small change in pH can result in unsuitable changes in the concentration of amine end groups in the polymer and fibre for those end uses where a high degree of uniformity of dyeing with acid dyes is required:

$$\begin{array}{lcccl} H_2N{-}(CH_2)_6{-}NH_2 & & H_3N^+{-}(CH_2)_6{-}N^+H_3 & & H[HN{-}(CH_2)_6{-}NHOC{-}(CH_2)_4{-}CO]_n{-}OH \\ + & \rightarrow & | \quad | & \rightarrow & + \\ HOOC{-}(CH_2)_4{-}COOH & & {-}OOC{-}(CH_2)_4{-}COO{-} & & H_2O \\ & & \text{AH Salt} & & \text{Nylon 6,6} \end{array} \quad [4.6]$$

For preparation of nylon 6,6 polymer, the salt solution is subjected to evaporation at boil, possibly at elevated pressures, until concentrations ≥60% are achieved. The concentrated salt solution together with a small amount (0.5%) of a molecular weight stabilizer is then heated in a reactor under a blanket of nitrogen so that temperature increases gradually and pressure reaches, typically, 1.73 MPa (250 psi). As water evaporates and temperature increases from about 212°C to 275°C, the molecular weight of the polymer reaches about 4000. Further reaction is achieved by a gradual decrease in pressure to atmospheric and then holding the polymer under these conditions for about one hour. At this point the polymer is not quite equilibrated but molecular weights are in the range of 12 000 to 17 000. The process is devised to remove all the liquid water present in the salt solution as well as almost all the potential water of reaction present in the form of carboxyl (–COOH) and amine ($–NH_2$) end groups with only minimal loss of the diamine (HMD) whose atmospheric pressure boiling point is 200°C. The molecular weight of the polymer is limited by the polymer-water-steam (vapour-liquid) equilibrium at atmospheric pressure. High molecular weight nylon for industrial applications is obtained by conducting the final stages of melt polymerization under reduced pressure or by addition of chain coupling agents. The finished polymer is then extruded in the form of a ribbon or strand, quenched with water and cut to form chips. After drying, the chips are sent for subsequent spinning operation. Alternatively the polymer may be sent directly to a spinning machine without prior solidification. In nylon 6,6 the polymerization reaction goes almost to completion. The formation of cyclic oligomers is less probable than for nylon 6 since the smallest possible ring is large, with 14 members for nylon 6,6, and the end groups are, consequently, less likely to approach

each other and react. Concentrations as low as 1–2% have been reported; this level is acceptable in fibres and therefore is not removed.[3]

This is represented by equation (3.29). The equilibrium constant of polyamidation reaction (equation 4.4) is shown in equations 4.5 and 4.7, where A is the concentration of amide groups (–CONH–) and P is the product of functional end groups (–COOH × $–NH_2$). For typically high extents of reaction and molecular weights, the value of the equilibrium constant (K) at 280°C is about 300 ± 50[4]:

$$K = A[H_2O]/P \qquad [4.7]$$

At high conversions the amide group concentration is almost constant as molecular weight varies, and the water concentration in the melt at a given temperature depends only on the water vapour pressure; the equilibrium value of P is proportional to water pressure. Deviation from this first power relationship is observed at high steam pressures and low molecular weights. The polymerization reaction follows second order kinetics at conversions up to about 90% and is not accelerated by catalysts.[5–6] However, at the higher conversions where molecular weights become of practical interest, the reaction becomes third order and it is catalyzed by –COOH end groups and other catalysts like hypophosphite salts or phosphonic acids.[7] The kinetic and equilibrium model for nylon 6,6 polymerization has been reported by Steppan and other researchers.[6] In addition to $–NH_2$ and –COOH end groups, the polymer may contain stabilizer or non-functional end groups which are introduced deliberately or produced by degradation.

4.3 Nylon 6

Nylon 6 can be considered to be the condensation polymer of ε-aminocaproic acid with a repeat unit of $–NH(CH_2)_5CO–$. In fact, this polyamide is almost always prepared from ε-caprolactam in a process which is essentially an additional polymerization. The advantages of this monomer are low cost and relative ease of purification compared with the amino acid. The pure monomer, which melts at about 69°C, does not polymerize when heated at elevated temperatures in the dry state. The key discovery (11)[8] that in the presence of both amine and carboxyl groups ring opening occurs readily, made possible the commercial processes for the polymerization of caprolactam. The simplest method is to carry out the polymerization[9] in the presence of water which hydrolyzes some of the lactam to form –COOH and $–NH_2$ groups which then catalyze the addition polymerization reaction. This can be accomplished at atmospheric pressure, but the times required to achieve equilibrium monomer content can

be greatly reduced by operation at elevated pressures and increased water concentrations.

The kinetic scheme for synthesis of nylon 6 includes following three main equilibrium reactions:

(a) Ring opening

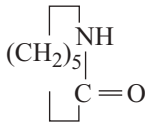

$$+ \; H_2O \rightleftharpoons HOOC — (CH_2)_5 — NH_2 \qquad [4.8]$$

ε-Caprolactam (CL) Amino caproic acid (P_1)

(b) Polyaddition

$$P_n + CL \rightleftharpoons P_{n+1} \qquad [4.9]$$

(c) Polycondensation

$$P_n + P_m \rightleftharpoons P_{n+m} + W \qquad [4.10]$$

where CL is caprolactam, W is water, P_n is polymer chain containing n repeat units. In addition, the formation of higher cyclic oligomers is an important side reaction. At equilibrium the presence of a significant concentration of the cyclic monomer along with lesser amounts of cyclic dimer and higher oligomers is known. For example,[2] the equilibrium concentration of caprolactam at 250°C is about 7.8% and of the dimer is 1.13%.

The ring opening reaction of caprolactam is endothermic and uses water to produce aminocaproic acid which acts as a monomer for other reactions. Therefore, the rate of this reaction depends upon the concentration of water in the mixture and temperature. Without an adequate amount of ring opening, rates of reaction are very low. In the polyaddition reaction, the monomer (CL) adds on the growing polymer chain and the equilibrium of this reaction alone decides the conversion of the polymerization reaction. The polycondensation reaction is responsible for the increase in molecular weight and produces water as a condensate product. The equilibrium of the polycondensation reaction decides the molecular weight of the resultant polymer. Both the polyaddition and condensation reactions are exothermic in nature.

As explained earlier the condensation polymers require to be stabilized for molecular weight to avoid post-polymerization during processing. As shown below, the incorporation of carboxylic acid-containing compounds can result in a polymer capped at one end due to reaction with stabilizer (monocarboxylic acids):

$$P_n + A_x \rightleftharpoons P_{nx} + W \qquad [4.11]$$

where A_x and P_{nx} represent a monocarboxylic acid stabilizer and the stabilized polymer, respectively.

Kinetics and mechanistic aspects of the polymerization have been reviewed in detail,[2,10–11] and the rate equations and kinetic and thermodynamic constants have been used successfully for simulation and control of the hydrolytic polymerization process.

Molecular weights of nylon 6 are generally in the same range as those of nylon 6,6. For nylon 6, a commonly used viscosity measurement for molecular weight involves use of a solution of 1 g of polymer in 100 cm^3 of 96% H_2SO_4. A value of 2.7 has been quoted[12] for polymer with $M_n = 20000$ and the value of α in the Mark–Houwink equation is 0.7. For melt viscosity, α was 3.5 and its low shear rate value was about 140 Pa s (1400 poise) at 280°C. For nylon 6 prepared as described above, the molecular weight distribution of the final polymer is the same as for other typical condensation polymers with $M_w/M_n = 1 + p$ or about two.

Factors influencing the polymerization and end product are temperature, water concentration and stabilizer-type and content.

4.4 Effect of temperature

As a consequence of the exothermic nature of the addition and condensation reactions, lower temperature is favorable for obtaining higher equilibrium values for both monomer conversion and degree of polymerization.

4.5 Effect of water concentration

From the mechanism and corresponding rate equation, it is readily seen that for a given temperature, the concentration of water affects the ring-opening and polycondensation reactions, and therefore, is the principal process parameter affecting both rate and attainable degree of polymerization. An increase in water concentration causes an increase in the ring opening reaction, creating more chains or end groups. The higher concentration of carboxylic acid groups is responsible for higher rates of reaction due their catalytic behavior:

$$\text{Rate constant } k = k_i^0 + k_i^c \text{ [concentration of end groups]} \qquad [4.12]$$

It must be noted that water has no bearing on the equilibrium conversion because conversion is controlled by polyaddition. With increase in water concentration the molecular weight goes down, because water is a by-product; equilibrium may be shifted to higher molecular weight only on removal of water.

4.6 Effect of stabilizer type and amount

Stabilizers block the functional groups; therefore excess of one functional group may result in stabilizing molecular weight towards the end. As mentioned above, the carboxylic functional groups catalyse the hydrolytic polymerization of nylon 6 (Equation 4.12). However, since monoacid or diacid stabilizers may provide additional COOH groups, rate constants for all polymerization reactions increase in the presence of stabilizer. In recent years diacid stabilizers have gained importance in nylon 6 polymerization because such monomers may be modified to contain sulphonic acid groups, which may be used as anionic dyesite for basic dyeable nylons. The diacid stabilizers are expected to provide higher level of catalytic activity in comparison to monoacid stabilizers. This favorably affects the reaction kinetics and reduces the cost of polymerization.

The kinetics of polymerization using both monoacid and diacid stabilizers have been studied by Agrawal and coworkers.[13,14] Using reaction kinetic calculations it was shown that in a closed isothermal batch reactor, the polymerization reactions proceed at a much higher rate in the diacid catalyzed system due to the presence of the two [═COOH] groups in its chemical structure. On the other hand, monoacid has only one [═COOH] group in its chemical structure, and therefore, shows lower catalytic activity. It is well known that the carboxylic (–COOH) groups catalyze all the kinetics reactions involved in the polymerization of caprolactam. Although both monoacid and diacid work as a stabilizer in controlling the molecular weight of the polymer at the end of the polymerization, the higher rates of conversion and molecular weight build up are observed in the case of diacid stabilized system.

Figures 4.1–4.3, respectively, show the comparison of the two systems polymerized at 265°C for build up of conversion, carboxylic groups, and amino groups with respect to the reaction time. It can be observed that from the beginning of the reaction, the concentration of the carboxylic end groups in the case of a diacid stabilized system is higher than in a monoacid stabilized system. The difference is maintained throughout the reaction and results in higher catalytic activity for all polymerization reactions. The concentration of amino end groups rises faster resulting in a peak occurring earlier to that in monoacid stabilized system. The concentration of amino end groups in case of monoacid stabilized system reaches maximum at about 1.0 h while in the case of a diacid stabilized system it is about 0.5 h. Table 4.1 shows that for both diacid and monoacid stabilizers, the conversion reached similar values, which confirmed that the conversion is independent of the type or concentration of stabilizer used.

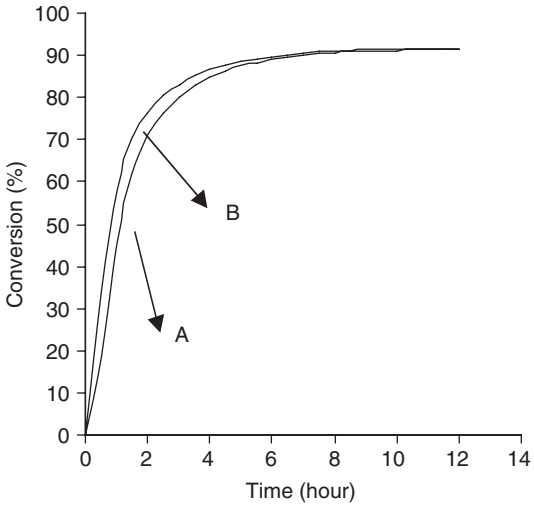

4.1 Comparison of conversion with time at 265°C for (A) mono and (B) diacid stabilized systems in closed isothermal batch reactor.

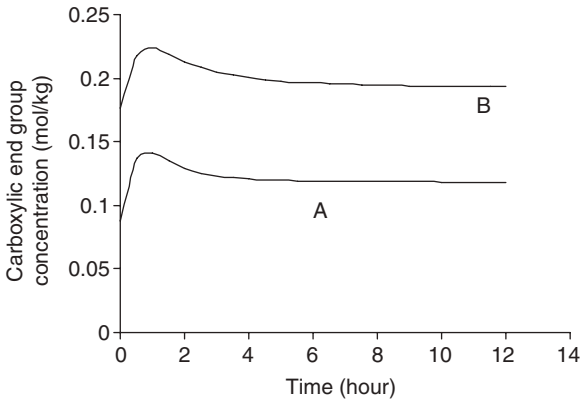

4.2 Comparison of total carboxylic end groups with time at 265°C for (A) mono and (B) diacid stabilized systems in closed isothermal batch reactor.

4.7 Reactor design

Nylon 6 polymerization may be carried out in a semi-batch reactor or a continuous tubular reactor (VK tube).

4.7.1 Semi-batch reactor

From the understanding of the factors affecting the kinetics of the polymerization reaction in nylon 6, it may be easy to infer that it is desirable

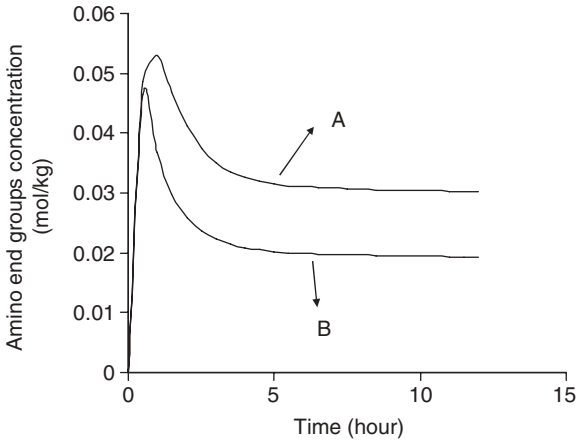

4.3 Comparison of amino end groups with time at 265°C for (A) mono and (B) diacid stabilized systems in closed isothermal batch reactor.

Table 4.1 Comparison of polymer properties in a closed isothermal batch reactor at equilibrium (more than 16 hours) for mono and diacid based stabilizers

Properties	245°C		255°C		265°C	
	Monoacid	Diacid	Monoacid	Diacid	Monoacid	Diacid
Conversion (%)	92.75	92.81	92.19	92.26	91.61	91.69
NAMW (g/mol)	8215.22	9126.18	8079.98	9011.94	7982.15	8937.68
[NH2] (/kg)	0.0256	0.0157	0.0268	0.0164	0.0275	0.0166
[COOH] (/kg)	0.1136	0.1917	0.1148	0.1924	0.1155	0.1926

to alter the condition of the polymerization during the initial and the final phases of the reaction. Initially, the water is kept high by applying high pressure in the reactor to facilitate ring opening reaction. Also the temperature of the reaction is kept high to allow rapid conversion of the monomer and build-up of the molecular weight. At the later stages, the reactor is slowly brought under low pressure and to lower temperature to favour high molecular weight and high conversion.

This scheme of polymerization may also be carried out in a semi-continuous manner by using a sequence of two semi-batch reactors. The first reactor should have a higher temperature and higher water concentra-

tion so as to achieve a rapid reaction rate and the second should have a low temperature and low water concentration in order to drive the polycondensation and polyaddition reactions in the forward direction to obtain high molecular weights and conversions.

4.7.2 VK tube

One of the popular reactors used in industries for the hydrolytic polymerization of ε-caprolactam is the VK (Vereinfacht Kontinuierliches Rohr) column reactor. VK column reactors are specially designed vertical tube reactors where internal gratings are placed in order to achieve uniform heating and near flat velocity profile of reaction mass.

The industrial VK tube reactor consists of several different zones, where the temperature is independently measured and controlled. A schematic representation of the reactor with five zones is given in Figure 4.4(A). Feed consisting of molten caprolactam, water and mono- or di-functional acid is fed under the nitrogen cover at the top of the column. The purged nitrogen is made to escape through a water seal located at the top of the reactor. The reaction mixture fills the entire tube and is heated in zone I as it passes through a heat exchanger I to a temperature of about 240°C. Thereafter (zone III upper and lower) the melt is heated by the heating jackets and the ongoing exothermic reactions. The temperature of the reaction mass gradually increases from the top to the middle zone till a highest temperature point (T_h) of about 260–270°C is reached. Thereafter, the temperature is decreased to 240–250°C using another heat exchanger and stabilized towards the bottom of the column using the jacket temperature. The products, polymer and unreacted monomer, are removed at the bottom of the reactor.

As stated above, ring-opening and polycondensation reactions are very sensitive to the water content in the reaction mass at any point. Use of water also affects the concentration of carboxylic end groups, which helps in catalyzing all the polymerization reactions. Therefore, water concentration profile in reaction mass along the axis of VK tube reactor significantly affects the end product properties.

In a VK tube reactor, large quantities of water are added to initiate the ring-opening reaction. The high temperature, at the top portion of the VK tube, readily evaporates the volatile components, water and caprolactam, until equilibrium is attained between the vapor and liquid phases. Evaporated caprolactam is condensed and returned back to the VK tube. Most of the added water is evaporated and removed as condensate within a short time after addition. As the reaction mass moves down the reactor towards the highest temperature point (T_h), more and more water is evaporated, and the vapor rises to the top surface of the reactor. This transfer

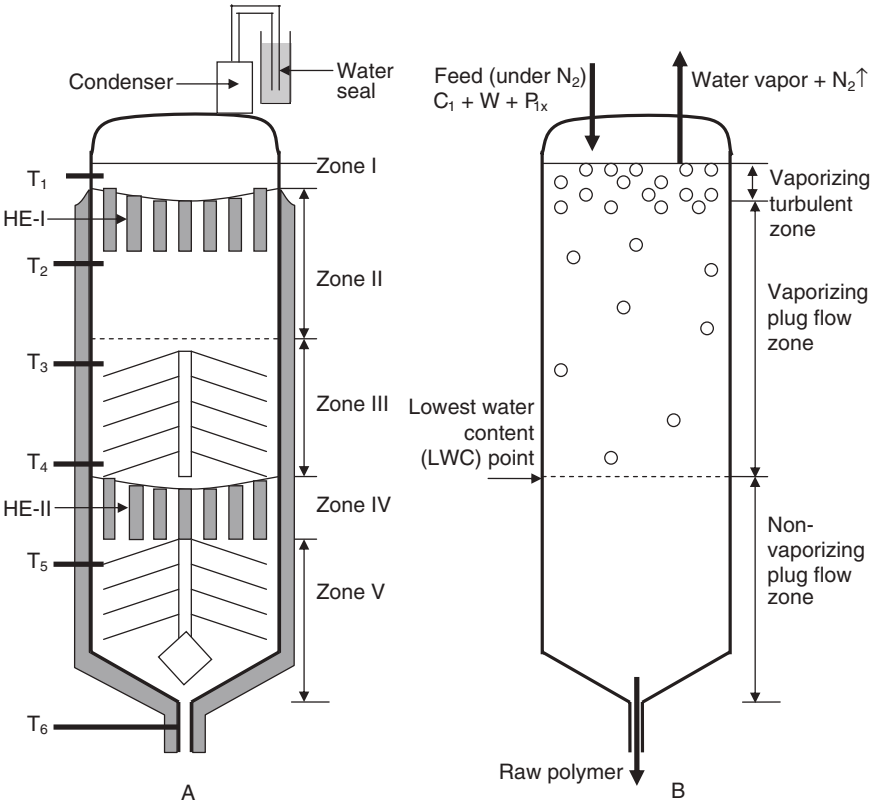

4.4 VK tube reactor: (A) Schematic diagram of industrial VK tube reactor depicting the various heating zones (zone I – zone V), heat exchangers (HE-I and HE-II) and temperature measuring points (T1 to T6); (B) VK tube reactor model consisting of three main zones: Vaporizing turbulent (top) zone, vaporizing plug flow zone and non-vaporizing plug flow zone.

of water vapor helps in maintaining both the liquid and vapor phases in near equilibrium state at all places in the upper portion of the reactor. This gradual evaporation of water due to rising temperature results in a 'lowest water content (LWC)' point.

Since the water can vaporize and escape by rising to the surface of the melt, the water content at any point in the reactor depends on the combined action of temperature and pressure till the lowest concentration of water is reached. Higher temperature tends to reduce water content whereas higher pressure increases it. This counteraction of the two parameters results in a point in the VK tube that is the 'lowest water content (LWC) point'.

When the reaction mixture crosses the highest temperature point (T_h), the lower temperature and higher hydrostatic pressure in the bottom portion of the reactor suppresses the vaporization of water, and the remaining portion of VK tube reactor is practically a non-vaporizing tubular reactor. Therefore, a VK column reactor can be considered as a reactor consisting of three main zones: at the top is a turbulent zone, which may be considered as a two-phase (gas-liquid) continuous stirred tank reactor (CSTR) type zone, a middle zone as a vaporizing plug flow tubular zone, and a bottom zone as a non-vaporizing plug flow tubular zone. The three zones are shown in Figure 4.4(B).

The VLE equation suggested by Fukumoto[17] for the end of polymerization under vacuum conditions has been found to be suitable for most of the vaporizing zone based on the comparison between the predicted and experimental values:

$$[W] = 10^{-2} P_T \exp\left(\frac{8220}{T} - 24.36\right) \qquad [4.13]$$

The prediction of polymer properties is improved by modifying the constants in the equation to account for the pressures higher than the atmospheric pressure condition inside the VK tube:

$$[W] = 10^{-2} P_T \exp\left(\frac{8220}{T} - 22.24\right) \qquad [4.14]$$

where P_T is the total pressure in Pascal defined by

$$P_T = P_A + 9.81(\rho_w H_w + \rho_m H_p) \qquad [4.15]$$

where P_A = atmospheric pressure = 1.013×10^5 Pa.

Equation 4.15 can be used for calculating concentration of water at every point in the vaporizing zone of the reactor. From the 'lowest water content (LWC)' point downward (i.e., non-vaporizing zone), the summation of water in the reaction mixture, i.e. [W], and the water which is part of the polymer i.e. [P], can be considered to be constant. The concentration of water [W] at any point in non-vaporizing zone is then estimated using a mass balance equation as follows:

$$[W] + [P] = [W_c] + [P_c] \qquad [4.16]$$

where $[W_c]$ and $[P_c]$ are the concentrations of water and polymer at the 'lowest water content (LWC)' point, respectively; [P] is the concentration of polymer at the point of consideration in the non-vaporization zone.

Figure 4.5 shows the temperature and pressure variation along the axis of a typical VK tube reactor. The pressure at any point inside the reactor

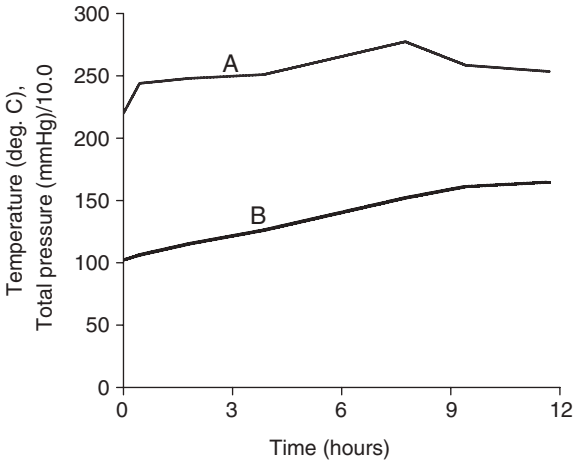

4.5 Typical profile of (A) melt-temperature (measured) and (B) total pressure (calculated) along the axis of the reactor versus reaction time.

is a summation of atmospheric pressure acting on the top of the reactor, head pressure due to the water seal length at the top of the reactor, and the hydrostatic pressure caused by the weight of the polymer mixture on the top of the concerned point. The pressure on the reaction mixture changes from 1.023×10^5 Pa at the top of the reactor to 2.082×10^5 Pa at the bottom of the VK reactor of about 10–11 m height. Besides the above, the flow of viscous polymer melt through the VK tube may also lead to pressure losses which need to be accounted for if large. However, such pressure losses are expected to be small and therefore can be neglected. The pressure variation is generally non-linear with the reaction time because the effective cross-sectional area of the reactor is different in different reaction zones.

The counter-flow direction of the rising water vapor in the vaporizing zones can cause some agitation of the reaction mass. Due to this reason, the earlier models of VK tube[11,16,17] assumed the vaporizing zones to behave like a CSTR and modeled the VK column reactor as CSTR (or a series of CSTRs) followed by a plug flow reactor. However, modeling the entire vaporizing zone of VK tube as a combination of CSTRs may be incorrect because significant agitation exists only in the top zone of the reactor. Figure 4.6 shows a profile of the water concentration inside a typical VK tube. It can be observed from the figure that the most of the water evaporates soon after it is added at the top of the reactor. This occurs within 0.5 hours of the start of the reaction. Therefore only this first 0.5 hours of the reaction may be considered as a CSTR.

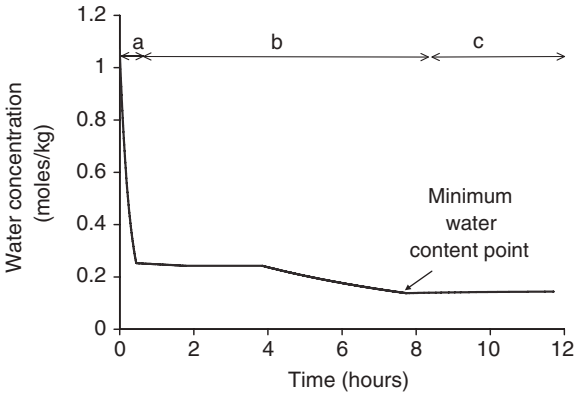

4.6 Typical profile of water concentration along the axis of the reactor versus reaction time: (a) turbulent vaporizing zone; (b) vaporizing plug flow zone; (c) non-vaporizing plug flow zone.

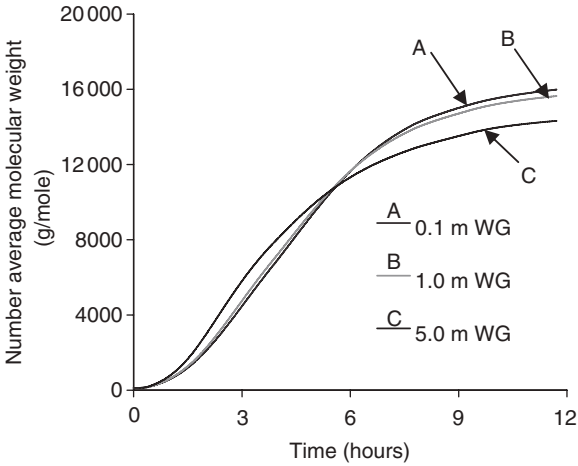

4.7 Effect of water seal length at the top of the VK tube reactor on number average molecular weight.

Effect of pressure in a VK tube

In a VK tube reactor pressure plays a crucial role. The increasing pressure inside the VK tube along with temperature define the concentration of the water available for the reaction. The pressure inside the VK tube may be altered by applying a static pressure at the top of the reactor. Figure 4.7 depicts the effect of head pressure (which is the pressure created by the water seal at the top of the VK tube) on the number average molecular weight of the polymer. As an example, increase in water seal length from

0.1 m to 5 m, results in significant improvement in the rate of reactions as more water may tend to stay inside the reactor. However, due to larger water content at the equilibrium, number average molecular weight decreases by about 10.5% and amino end groups increase by about 15.5%.

Effect of temperature profile in the VK tube

The temperature profile in the VK tube reactor is another important parameter in optimizing reactor performance. It is important that the temperature of the reaction mass is first increased slowly to the highest temperature point and then decreased to the final desirable temperature of equilibrium. This profile helps in first retaining the water for proper initiation of the reactions and later allows removal of water to the desirable extent at the highest temperature point. Water content at the highest temperature point ultimately decides the water content at the end of the reaction, and thereby, the properties of the polymer.

The temperature at the 'highest temperature point (T_h)', therefore, plays an important role in deciding the polymer properties. When the highest temperature is allowed to increase, the water content at the lowest water point decreases. This decrease in [W] in the non-vaporizing zone, increases the number average molecular weight as depicted in Figure 4.8. The calculations show that with a nominal change of the highest temperature (T_h) by 10 K, the molecular weight changes significantly by about 11.5%.

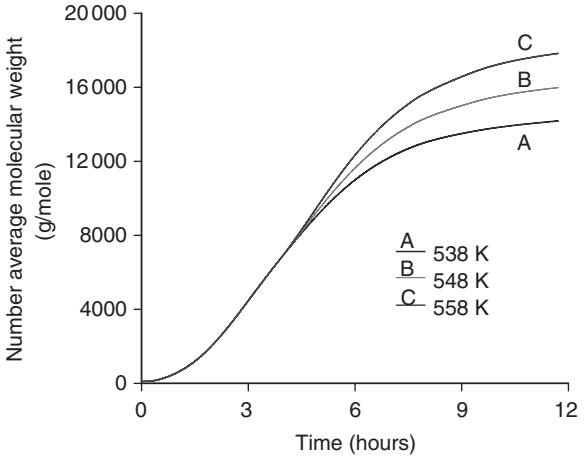

4.8 Effect of the highest temperature (T_h) on the number average molecular weight.

Effect of stabilizers

In a VK tube reactor, the use of diacid stabilizer over monoacid stabilizers also brings in substantial change in the kinetics of the reaction and the overall reaction time. Due to higher rates of reactions, diacid stabilized system achieves equilibrium faster than monoacid stabilized system and results in shorter polymerization time by 20–25%.[15,16]

Effect of internal design of the VK tube

It is important to control both the pressure and temperature profiles in a VK tube reactor in order to achieve desirable reaction time. It is desirable to have high pressure at relatively high temperature in the vaporizing zone. This would allow polymerization to reach equilibrium at a faster rate. Eventually, added water may be removed to the desired extent by increasing the temperature at the highest temperature (T_h) point before cooling the reaction to a lower temperature in the non-vaporizing zone. However, in a conventional VK tube, the possibility of increasing T_h is limited by the low heat-removal capacity of the reactor. Uncontrolled heat generation at the center of the reactor due to fast exothermic reactions at high temperature may result in gelling or degradation of the polymer. This limitation may be overcome by providing an efficient cooling device such as an additional heat exchanger just above the highest temperature point. This would allow controlled polymerization at the desirable temperature profile.

Other variations in the designs of VK tube involve a gas purging device at the end of the vaporizing zone to control the concentration of water at the lowest water content point. For industrial nylon 6, the molecular weights may be increased by adding a vaporizer.

Conversion of monomers in VK tube

Although it is not necessary to reach an absolute equilibrium in nylon 6 polymerization, near equilibrium conditions are desirable for a stable system with dependable results. The extent of a reaction may be determined by studying 'Ψ_i factor', which is defined for a reaction 'i' by the following expression:

$$\Psi_i \text{ factor} = (R_{if} - R_{ib})/R_{if} \quad i = 1, 2, 3 \qquad [4.17]$$

where R_{if} and R_{ib} are forward and backward rates of reaction for a given reaction 'i'. A reaction reaches equilibrium when the 'Ψ_i factor' becomes zero, in other words, the forward reaction rate becomes equal to the backward reaction rate. The 'Ψ_i factor' versus reaction time for all the

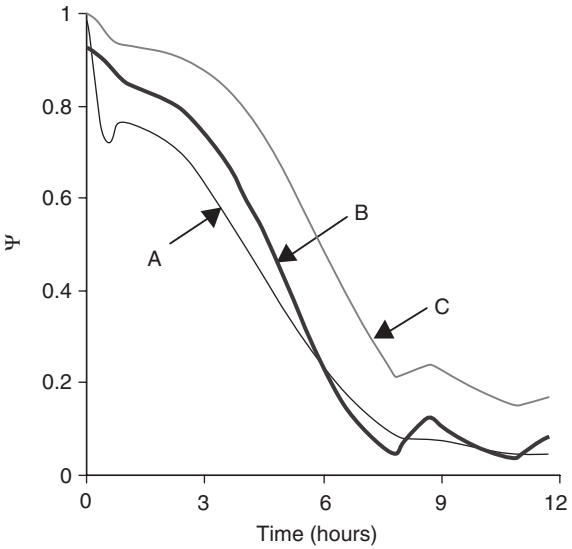

4.9 Values of 'Ψ' factor for the three major reactions versus reaction time in a typical VK tube: (A) ring-opening reaction; (B) polycondensation reaction; (C) polyaddition reaction.

major reactions – ring-opening, polycondensation and polyaddition are plotted in Figure 4.9 for an experimental case. It is interesting to note that all reactions show a similar trend. Initially at the start of polymerization, all reactions show $\Psi_i = 1$ as there is no possibility of backward reaction. The 'Ψ_i factor' decreases with time for all reactions, except for the ring-opening reaction, which shows a sudden increase in Ψ at about 0.5–1 h. This increase in Ψ_i may be due to a lower rate of backward reaction as aminocaproic acid is utilized by the other two reactions. All reactions tend to reach equilibrium together at about 7–8 h. However, Ψ values for polycondensation and polyaddition reactions increase when the reaction equilibriums are disturbed favorably by lowering the reaction temperature in the non-vaporizing zone. However, ring-opening reaction continues its downward trend at this zone since it is an endothermic reaction.

Net rates for all reactions start to increase almost simultaneously. The maximum value for the net rate of reaction for ring-opening occurs at around 2.3 h followed by polyaddition at around 2.8 h and finally polycondensation at 3.4 h. The peak values for all the three reactions occur at reaction times that are close to each other and are within the initial 30% of the overall reaction time. The rate of reaction for polyaddition is higher than those of the other two by about one–two orders of magnitude. From Figure 4.10, it can be seen that curve of polyaddition overlaps the curves

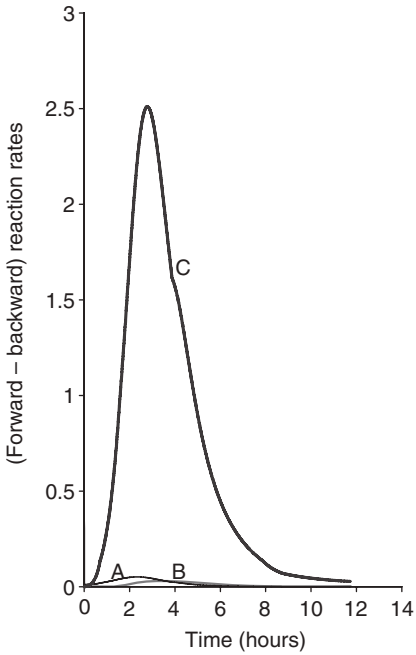

4.10 The variation of net rates of reaction (= forward – backward reaction rates) for the three major reactions versus reaction time in a typical VK tube: (A) ring-opening reaction; (B) polycondensation reaction; (C) polyaddition reaction.

of ring-opening and polycondensation from the beginning to the end of the reaction.

The concentration of functional end groups also changes with reaction time (Figures 4.11 and 4.12). The end group concentration is maximum at around 4 h due to the higher rate of ring-opening reaction than polycondensation. Thereafter, polycondensation rate predominates (Figure 4.10) over the former and results in the decrease of end group concentration. All this time polyaddition is the fastest reaction of all, helping to improve the molecular weight of the polymer at a slow and steady pace. However, it must be kept in mind that increase in molecular weight is rather poor with polyaddition reaction. The final molecular weight is achieved only because of polycondensation reaction.

4.8 Synthesis of modified polyamides (nylon 6)

Nylon 6 may be modified during the polymerization with comonomers or stabilizers to introduce new functional groups or chain end groups and thus

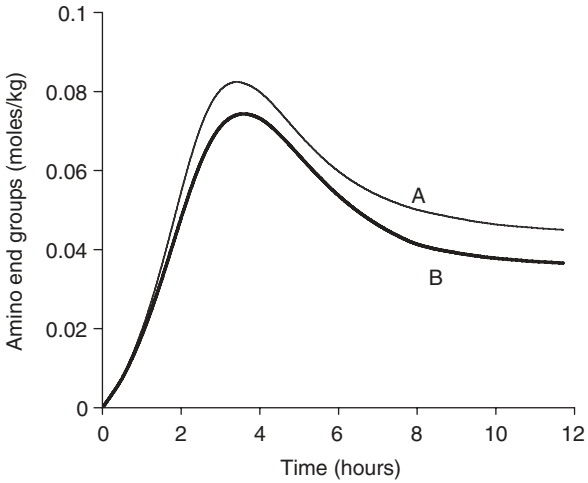

4.11 Calculated amino end group [NH_2] concentration in a typical VK tube: (A) considering the effect of increasing hydrostatic pressure inside the reactor; and (B) assuming constant atmospheric pressure throughout the reactor.

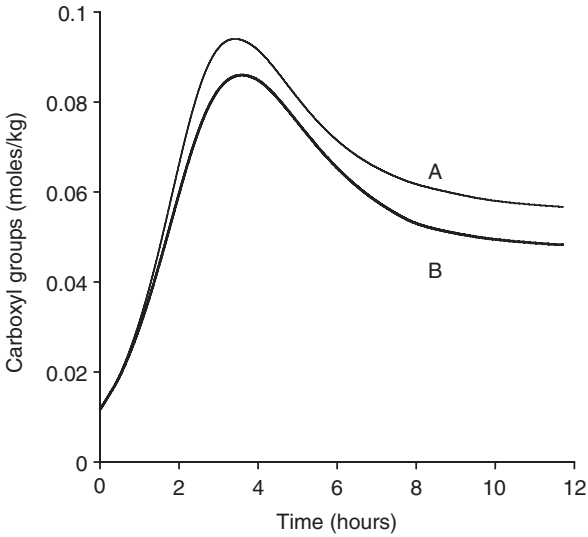

4.12 Calculated carboxylic acid end group [COOH] concentration in a typical VK tube: (A) considering the effect of increasing hydrostatic pressure inside the reactor; and (B) assuming constant atmospheric pressure throughout the reactor.

change the reactivity and chemical properties such as dyeability. In addition, the polyamide fibres can also be subjected to a variety of treatments including chemical, grafting, radiation, and plasma which alter the surface characteristics of these polymers.

Various nylon 6 nanocomposite polymers have been synthesized by in situ polymerization ε-caprolactam in the presence of nanomaterials.[18–21] Nylon 6/nano-TiO_2 and nylon 6/nano-Al_2O_3 composites have excellent photooxidative degradation resistance.[18,19] In the presence of pristine and carboxylated multi-walled carbon nanotubes (MWNT and MWNTCOOH) both the storage modulus (E′) and glass transition temp. (T_g) of the PA6/CNTs composites increase significantly.[20,21]

4.9 Modification at polymerization stage

Nylon 6 may be modified during polymerization by introducing small amount of a comonomer containing desirable functional side groups.

Since $-NH_2$ and –COOH are the functional groups involved in the polymerization reactions, a comonomer may be added with the following general chemical formula for synthesizing a copolymer with nylon 6:

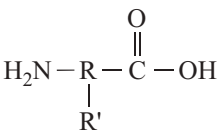

Alternately, two monomers may be added in equal molar ratio as given below:

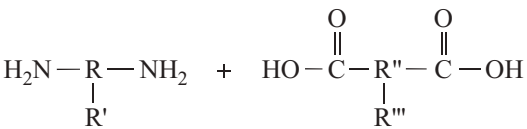

Apart from using comonomers to introduce new functional groups, stabilizers such as monoacids, monoamines, diacids or diamines, may also be used for introducing desired functionality to nylon 6. These stabilizers modify the end groups of the polymer chains and thus change their reactivity and chemical properties such as dyeability:

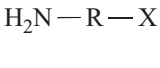

Monoamine

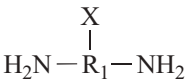

Diamine

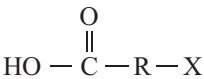

Monoacid

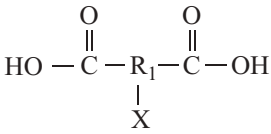

Diacid

Another approach that is used for modifying nylon 6 is by transamidation reaction. In this method, the tendency of polyamides to break and reform their amide linkages is utilized. After breakage, the amide linkage may reform with a free amine of any available polyamide segment. A typical representation of such reaction is:

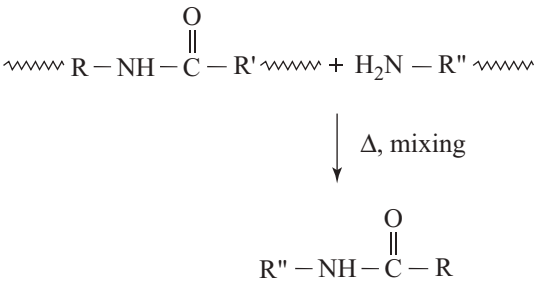

Using the above reaction mechanism, a new group R″ is readily introduced in nylon 6 by mixing another suitable polyamide containing R″ at the polymerization temperature. Since the above exchange occurs randomly at any amide linkage, initially after lapse of short reaction time, the two polyamides react to give a block copolymer with segments of each polyamide. If the transamidation is allowed to continue for a longer time then these segments further undergo amide exchange and eventually result in a random copolymer as shown in Figure 4.13. Therefore, care must be taken to arrest the reaction at an appropriate time so that only the desired amount of segmental exchange takes place. A completely random

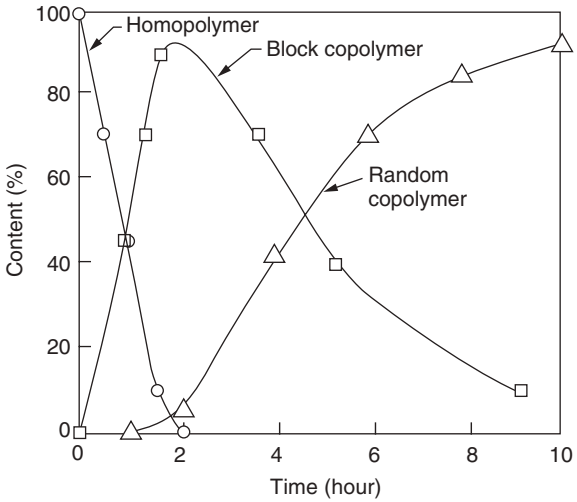

4.13 Conversion of two homo polyamides via amide interchange to block and random copolymer with time.

copolymer will not be suitable to form fibres as it would not be able to crystallize.

4.10 Dyeability of nylon 6

ε-Caprolactam, if allowed to polymerize without the use of a stabilizer, results in a polymer with equal numbers of $-NH_2$ and –COOH groups. For a polymer of about 16000 g/mol molecular weight, end group concentration is about 62 eq/ton for each type of the two end groups. Addition of a small quantity of stabilizer such as acetic acid blocks some number of NH_2 groups and helps in producing nylon 6 with normal dyeability, where an NH_2 end group concentration of about 35–45 eq/ton is targeted. Since NH_2 groups are the reactive functional sites for attracting acid dyes, any variation in amino end-group concentration changes the dyeing characteristics of the resulting fibres. If more NH_2 groups are blocked by adding a little more monoacid or a diacid such as sebasic acid, then dyeability of nylon with acid dyes may decrease substantially. A concentration of 10–15 eq/ton of NH_2 groups in the final polymer results in light dyeable nylon 6.

Similarly, if the concentration of NH_2 groups is increased beyond 40 eq/ton to the values of 80–90 eq/ton, deep dyeable nylon 6 is achieved. This increase in NH_2 concentration may be obtained by adding required quantity of diamines in place of mono or diacid as stabilizers:

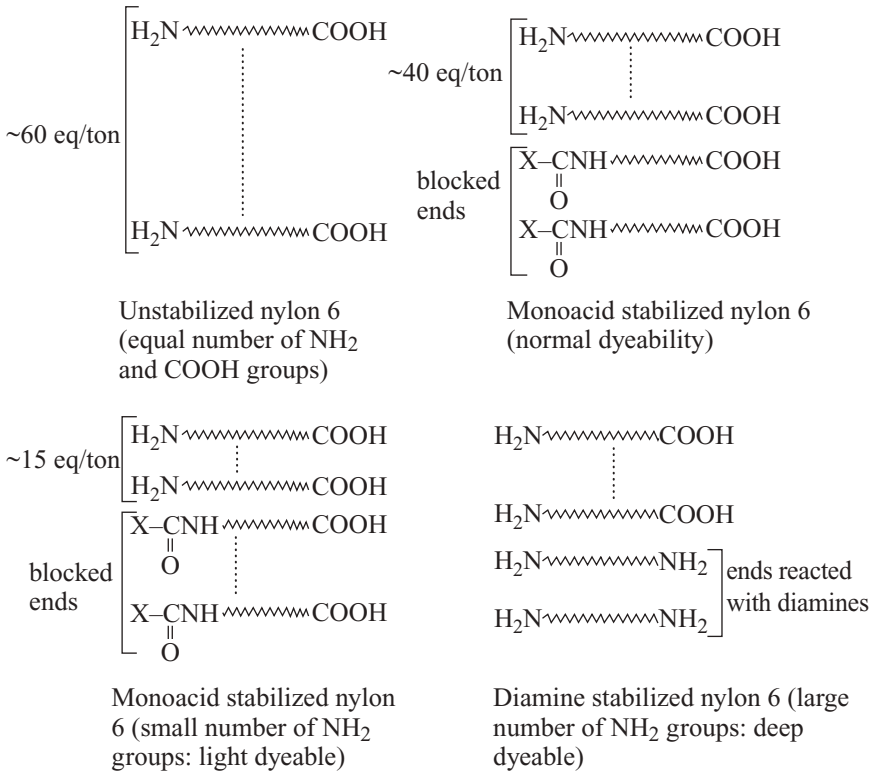

Diamines stabilize the molecular weight by reacting at the –COOH end group, and altering the 1:1 ratio of amino and carboxylic end groups. However, in doing so they convert the –COOH end group to an additional NH_2 end group. This results in a much higher concentration of NH_2 end group than possible with unstabilized/unmodified nylon 6:

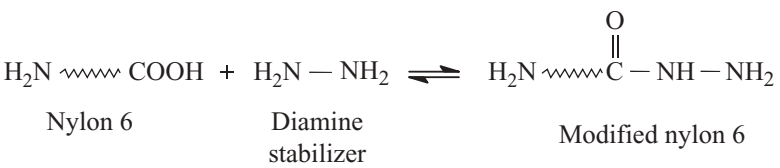

The dyeability of nylon 6 may be further enhanced and grades such as ultra deep (with NH_2 = 95–100 eq/ton) and super ultra deep (with NH_2 = 115–130 eq/ton) may be produced using a greater quantity of diamines to block additional –COOH end groups mentioned above.

The addition of a much higher quantity of stabilizers either mono/di acids or diamines for obtaining required dyeability characteristics places

stringent regulations on polymerization process. Obviously, the molecular weight of modified polymer may become substantially lower if the condensation reaction is not pushed forward by removing additional quantity of free water. Alternately, dyeability of the nylon 6 may be modified by adding a second polyamide flake of the same polymer type but adding a different amine end level to the extruder with the first polyamide flakes. This is followed by mixing and melting the two flakes under specific conditions to produce a blend with the required concentration of amino end group.

4.11 Cationic dyeable nylon 6

Nylon 6 is principally dyed using only the acid dyes as amino groups are highly active dye sites. The other functional group, carboxylic end group, forms only a weak acid group and therefore cannot attract basic or cationic dyes in normal nylon 6. For achieving cationic dyeability, stronger functional groups such as sulphonate acid groups are required to be introduced during polymerization. Use of modified stabilizer containing cationic dye sites has been suggested. Disodium 3,5-disulphobenzoic acid with following structure may be used as the stabilizer to the extent of about 1 wt% on caprolactam[22];

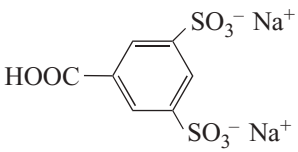

The above molecule reacts at the amino end group and provides two sulphonate groups as shown below:

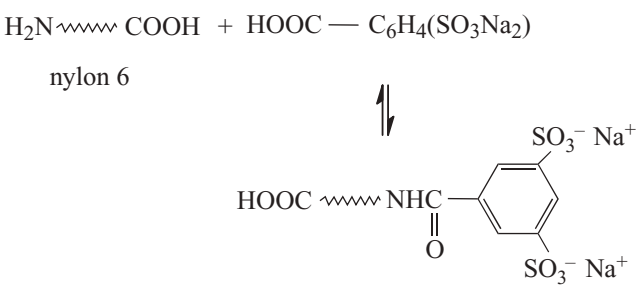

Cationic dyeable nylon 6 is normally less receptive towards acid dyes as amino groups are sacrificed in favour of sulphonate groups. Cationic dyeable nylon 6 may also be produced by adding 1–5% sulphonated diamino stilbene[23] during the synthesis stage. It is also possible to produce a

copolymer by adding a dicarboxylic acid monomer in addition to the above diamine mentioned. The mechanical properties of the modified nylon 6 may be improved but the improvement depends upon the concentration of comonomers used.

4.12 Antistatic and hydrophilic nylon 6

Nylon 6 has a moderate moisture regain of about 4–4.5% at standard condition. This is significantly better than many synthetic polymers such as polyesters, polyolefins, etc., however, still it is lower than many of the natural fibers such as cotton, silk or wool. The comfort properties of a fabric depend on several attributes of which moisture absorbency is one of the most important properties for applications related to innerwear and sportswear. The moisture wicking property of fabrics, which contributes towards comfort value under heavy perspiration conditions, has been found to be higher for more hydrophilic fibers than hydrophobic fibers.[24]

Moisture regain in nylon 6 is due to the presence of hydrophilic amide linkages. If hydrophilic groups per unit weight of the material could be increased, then it would lead to higher moisture content at the standard conditions. For example, nylon 4, which has a higher concentration of amide linkages in the polymer mass, shows 9.1 wt% moisture regain. Based on similar reasoning nylon 6 is made more hydrophilic by copolymerizing the polymer with copolymer segments containing hetero atoms such as ether links of poly(ethylene glycol) segments[22] having the structure shown below:

$$H_2N{-}CH_2{-}CH_2{-}CH_2{-}O{-}(CH_2{-}CH_2{-}O)_n{-}CH_2{-}CH_2{-}CH_2{-}NH_2$$

Diamine functionality is used in such comonomer segments to facilitate copolymerization with carboxylic acid end groups of nylon 6 chains. This gives block copolymer structure. Random copolymerization using small polyether molecules is not advisable as it may lead to formation of essentially amorphous material, which is unsuitable for fiber formation.

Example of such a hydrophilic nylon 6 fiber is 'Hydrofil' developed by Allied Fibers.[24] This fiber is obtained from a block copolymer of nylon 6 and polyethylene glycol with about 15% PE and rest nylon 6. At standard conditions of 65% relative humidity and 70°F temperature, the fiber has moisture regain of about 5.4% which increases to about 14.4% at 95% RH and 90°F (32°C) temperature. The moisture absorption at higher relative humidity compared well with that of cotton. The material is suitable for making active wear fabrics. Alternately, a copolymer of adipic acid-caprolactam-polyethylene glycol[25] may be used as an additive in the nylon 6 matrix to impart antistatic properties even at a relative humidity below 45%.

Hydrophilic segments such as polyether-amides may also be introduced by transamidation. The fibers produced from such composite materials have lower crystallinity and higher moisture regain. Initially, on the physical mixing, the two polyamides are in separate phases, however as time proceeds, mixers of molten polyamide undergo transamidation (amide interchange) reaction to form a block copolymer. Vivrelle polymer developed jointly by Sun Co. and SNIA fibers[26] is an example of such a block copolymer.

4.13 Flame retardant nylon 6

Nylon 6 can catch fire in normal atmosphere as its Limiting Oxygen Index (LOI) is around 21. However, it has self-extinguishing properties due to its extensive shrinkage and dripping behavior during combustion. When the nylon polymer is ignited, it melts and then the molten polymer drips away from the flame. However, if the molten polymer is not able to escape fire, then it propagates fire. The nylon 6 can be rendered flame retardant by either using certain phosphorous/halogen based comonomers during polymerization or by adding flame retardant additives during melt spinning.

Bis(2-carboxy ethyl)methyl phosphine oxide (CEMPO)[27] when used as a comonomer with hexamethylene diamine (HMDA) gives a flame retardant copolymer fiber with LOI of ~25%. The fibre properties are not significantly affected up to a concentration of 35 mol% of CEMPO. The chemical structure of the additive is:

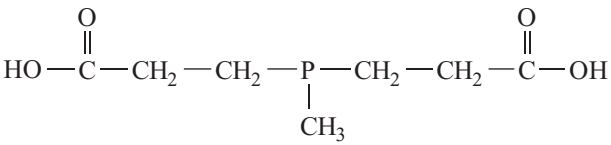

(CEMPO)

Net phosphorus content of about 1.5 wt% on polymer weight gives adequate protection against fire. Halogen based monomers or additives, though effective, are no longer recommended because of the emission of halogen acid during burning. Vapours of these acids may cause personal injuries.

4.14 Elements of melt spinning process of nylons

A fiber or a filament (a continuous form of fiber) is the fundamental unit of textile materials. It has high strength (tensile, bending, torsional, or

compression), high flexibility (i.e. low moduli), extensibility, and shows recoverability on deformation. Most of these properties are observed about one principal direction, which is known as the axis of the fiber. Since all textile structures – one to three dimensional (yarn, fabric, or braids, etc.), are built using this basic structural unit, these structures also possess such unique properties.

In order to possess such properties, the fiber or filament has a unique micro-structure (morphology) in which majority of the polymer chains are oriented in the direction of the axis of the fiber. The more oriented the polymer molecules are in this direction, the better properties the resulting fiber/filament is considered to have. For producing man-made fibers, the polymers (either natural or synthetic) must be unfolded and extended uni-directionally to extremely large dimension to get high aspect (length to diameter) ratio and high orientation. This is known as spinning.

In spinning, a small amount of polymer (say ~1 g) may be elongated to over 9000 km while the other dimension (diameter) is only in microns. This requires a precise control over the spinning process to enable such unidirectional extensions in melt form. In fiber formation, all efforts are directed in controlling the microstructure of the polymer so that properties as mentioned above are obtained with respect to the principal axis of the fiber. This is unlike other methods of polymer processing such as injection molding, compression molding, extrusion and blowing, etc., where mostly isotropic properties are desired and only a little attention is directed in making a controlled microstructure in terms of molecular orientation and their spatial arrangement.

In spinning, polymer melt or solution is extruded from a fine hole and is elongated by applying a tensile external force on the extruded portion. As the polymer melt or solution is pulled, it is cooled or precipitated, respectively, to form a solid filament. This filament is then usually subjected to post-spinning operations such as drawing, which is unidirectional stretching in a semi-solid form, and heat-setting, which is crystallization to equilibrium. Other post-spinning processes, such as texturing, simply are variations of the drawing and heat-setting processes to impart curvilinear shape to an otherwise straight filament. This gives physical bulk to the filaments. The process of fiber formation is complete only when both spinning and post-spinning operations are carried out.

When polymer is moving inside a confined geometry, it is under a shear flow such as through a pipe or spinneret hole. During this flow, the molecules of the polymer do not orient significantly and the shear flow does not contribute to formation of fiber in typical nylons. However, liquid crystalline polymers may be transformed and oriented during a shear flow through a spinneret. In a flexible chain polyamide, the spinning and structure formation takes place only after the polymer melt has been extruded

through the spinneret. As the polymer comes out from the confined channels into the open atmosphere, i.e. extruded from the spinneret, its flow behavior changes. It is said to undergo elongational flow under tensile forces.

In an elongational flow, polymer fluid flows with a uniform velocity profile perpendicular to the direction of fluid flow. However, it may accelerate, or at other times, decelerates as it travels along its path. Most of the spinning is said to occur due to the elongational flow where fluid velocity keeps on increasing down the spinning line, resulting in unfolding of the polymer chains.

4.15 Structure development during melt spinning of polyamides

4.15.1 Spinning at low speeds

At lower spinning speeds, stress induced crystallization is absent. Therefore, with increasing level of spinning stress, the orientation of the polymer chains increases. However, it does not have any significant effect on crystallization.

Temperature profile changes both the orientation and crystallinity of the spinning filament. Higher temperature increases the spinning length (time spent by the spinning filament in spinning line) as the filaments take longer to cool down. It tends to increase polymer chain relaxation, and therefore, lowers the orientation. At the same time, the crystallinity of the filament increases because it spends longer at a higher temperature.

The winding (spinning) speed is critical in deciding the level of spinning stress inside the spinning filament. The stress in turn regulates the velocity gradient profile of the spinning line. Velocity gradient profile is the change in velocity of the filament with spinning distance. Below a critical stress level, the velocity gradient profile is a bell shaped curve as shown in Figure 4.14. The maximum velocity gradient is obtained somewhere in the middle of the spinning line and its maximum value increases gradually with the increasing spinning speed. The orientation in the spun filament is the function of this maximum velocity gradient value, i.e. the maximum strain rate.

The temperature of the spinning line also depends on the spinning speed.[28] At higher spinning speeds, the temperature of the spinning filament may be at a slightly lower temperature. This may be due to the enhanced cooling effect of the quench air at higher relative speed of the filament.

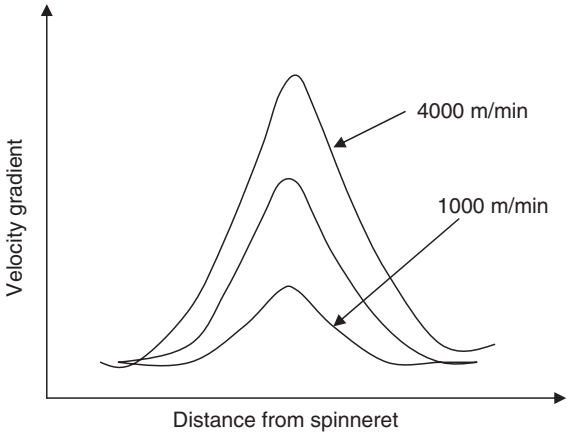

4.14 Effect of spinning speed on velocity gradient and temperature profile of the spinning filament at low speeds.

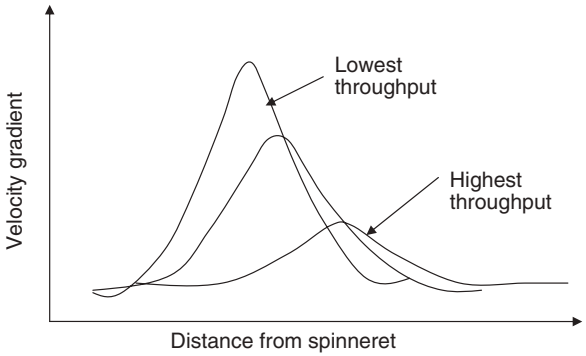

4.15 Effect of throughput on velocity profile and temperature profile of the spinning filament at low speeds.

Throughput also has significant effect on the temperature, stress, and velocity gradient profiles. With higher throughput, the value of maximum velocity gradient decreases and it maximizes at a later distance from the spinneret. This is shown in Figure 4.15. At higher throughput, the temperature of the filaments remains at a higher temperature for a longer time.[28] This is because with higher throughput (W), more heat comes into the spinning line and it takes longer for the same cooling system to cool down the fiber to its T_g. Therefore, not only does the overall temperature of spinning line increase, but the spinning length increases. The spinning fiber spends longer in the spinning line. The spinning length is defined as the distance traveled by the extruded fiber before it reaches a temperature below its T_g. Below T_g, the spinning is considered to be finished because

the fiber enters the glassy state and can no longer be stretched under the applied stresses.

Similarly, cooling air conditions have direct effect on temperature profile of the spinning filament, and therefore, on spinning stress. If the relative humidity of the cooling air is high, it can carry more heat due to its high heat capacity and provide better cooling to the filament. On the other hand, if the spinning polymer is sensitive to moisture such as polyamides, the moist air may act as a plasticizer and influence the T_g of the polymer. This will tend to lower spinning stresses (lower orientation), but facilitate crystallization at the same time. Therefore humidity of cooling air in such systems is regulated to towards lower value. Table 4.2 summarizes the effect of spinning parameters (assuming that only one parameter is being changed at a time) on the structure of the as-spun fibers at low spinning speeds.

4.15.2 Spinning at high speeds

As the spinning speed is increased further to higher values, the effect of air drag and inertial forces increases substantially on the total stress value of the spin-line. Many studies have been reported in the literature on modeling of the high speed spinning process to explain the spin line dynamics.[29–34] Figure 4.16 shows the effect of the spinning speed on the developed stresses of the spinning line in nylon 66.[30,35]

When these stresses cross a critical stress level, which is unique for a particular polymer, the polymer starts to undergo fast deformation (high strain rate) and the stress level rises rapidly due to diameter attenuation. At the high strain rate, its apparent elongational viscosity starts to decrease rapidly due to strain thinning, which further induces even faster deformation. This is known as region of 'super drawing' or 'necking'. This deformation cycle continues till polymer chains are pulled into high orientation and their degree of freedom is locked due to initiation of crystallization. This is known as stress-induced crystallization. The oriented and partly crystallized polymer chains turn into a rubber like structure and start to show strain-hardening behavior, which arrests further deformation of the structure. On strain hardening, the apparent viscosity starts to rise very sharply. This phenomenon is predicted in Figure 4.16 for nylon 66 case. At higher spinning speeds, the initial drop in the apparent viscosity is higher and faster followed by even faster rise after the stress-induced crystallization takes place. The freeze point is achieved soon after this strain-hardening phenomenon takes place. In contrast, no such changes in apparent viscosity are seen in the case of 1000 m/min of spinning speed.

The higher spinning speeds give rise to the higher necking tendency, which leads to more orientation and higher crystallinity. With higher

Table 4.2 Effect of spinning parameters on the structure of as-spun fibres

Parameter	Effect on spinning stress	Effect on filament temperature	Time spent in spinning line	Fibre orientation	Fibre crystallinity	Remarks
↑Winding speed	↑	↓	↓	↑	↓	
↑Throughput	↓	↑	↑	↓	↑	Higher denier
↑Cooling air temp	↓	↑	↑	↓	↑	Slower cooling
↑Cooling air speed	↑	↓	↓	↑	↓	Faster cooling
↑RH (hydrophobic fiber)	↑	↓	↓	↑	↓	carries more heat
↑RH (for hydrophilic fibre)	↓	↓	↑	↓	↑	Moisture plasticizes the polymer

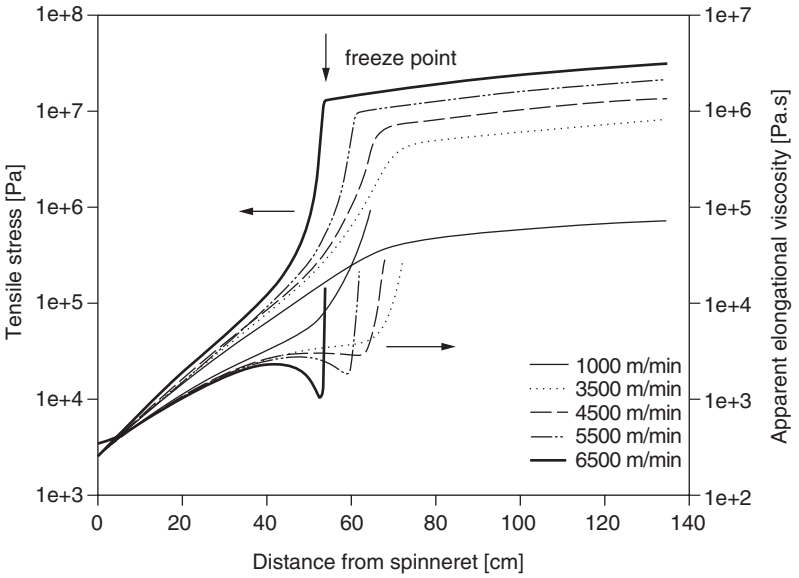

4.16 Effect of take-up speed on the tensile stress and apparent elongational viscosity profiles at constant mass throughput.

Table 4.3 Effect of spinning speed on the temperature of the spinning melt at which necking starts

	Temperature (°C) at the start of the neck					
Take-up velocity (m/min)	2000	3000	4000	5000	5500	6000
Polymer						
PP		67	114	114		
Nylon 12		90	102	135		
PET				102	123	148

spinning (winding) speed, the neck moves towards the spinneret and the change in velocity gradient is much steeper. The spinning is completed much sooner with the spinning path considerably reduced. Table 4.3 shows that the necking starts at a higher temperature at higher spinning speed for the three polymers studied.[36] The polymer spends a very little time in the necking region. It is predicted that necking in nylon 66 occurs for only 8–10 cm at 5500–6500 m/min and the time spent by the polymer in the neck region at these speeds is only about 5 ms. The stress induced crystallization as observed above may take place only if two parameters are favorable – the induction time for crystallization (i.e. inverse of nucleation

rate) and the rate of crystallization (i.e. rate of crystal growth). For an effective stress-induced crystallization to occur at higher spinning speeds, the induction time for crystallization should reduce and rate of crystallization should increase for the spinning polymer. In other words, the overall rate of crystallization should increase.

In nylon 6, the POY speeds are nearly 4000–4200 m/min. Nylon 6 spun at lower speeds undergoes post-spinning crystallization on conditioning. Therefore, it is difficult to obtain amorphous nylon 6 at any speed due to this phenomenon. At speeds near to 4000 m/min, nylon 6 POY is stable and essentially consists of γ crystals, which are deformable during drawing and texturing.

4.16 Spinning of nylon 6

In the spinning thread, in the absence of crystallinity, the polymer behaves as a single phase rubber-like network, adhering to affine deformation similar to spinning of PET. Due to a post-crystallization process that occurs after winding and conditioning, nylon 6 fibers develop a substantial level of crystallinity (50% or more) even at low wind-up speeds. The developed crystals are of α type. The structure of the amorphous network developed in the spinning thread is preserved in the final wound sample in spite of post-crystallization. The orientation of the crystalline phase that develops during post-crystallization is relatively high even at low wind-up speed. Apparently, post-crystallization starts from highly oriented amorphous segments, such as short network chains that become fully extended at low overall network deformation. Post-crystallization leads to a pronounced difference in birefringence determined on-line and after winding.

The change in birefringence on conditioning is indicative of the degree of instability the as-spun material shows (Figure 4.17).[37] Upon conditioning, the fiber spun at low spinning speeds extends owing to crystallization, which throws the molecular chains in the axial direction. At a speed of 2000 m/min, the extension is the maximum while it reduces slowly to a negligible value as the spinning speed increases to about 4000–4200 m/min. At this speed, the extension due to crystallization and contraction due to residual spinning stresses are well balanced. At spinning speeds higher than 4200 m/min, the as-spun fiber shows net contraction, which increases slowly with increasing spinning speed.[38]

Figure 4.18 shows a series of true stress–strain curves for undrawn yarns obtained over a wide range of wind-up speeds (500–6500 m/min), that have been shifted horizontally to coincide with the 500 m/min LOY curve. For yarns spun at wind-up speeds below 4000 m/min, a good fit with the mastercurve is obtained. For yarns spun at wind-up speeds above

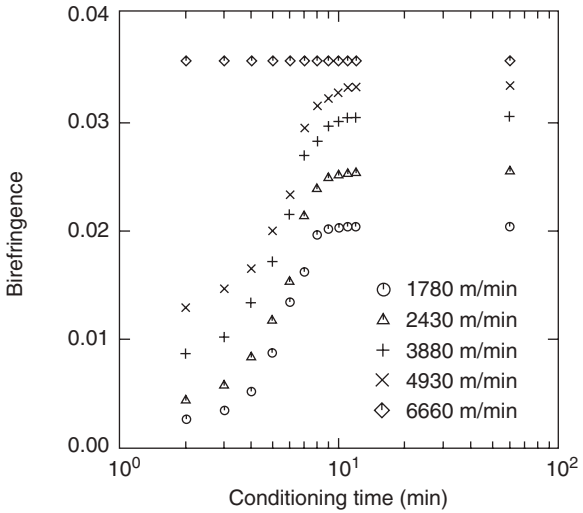

4.17 Change in birefringence with conditioning time of nylon 6 with a mass throughput of 2.99 g/min.

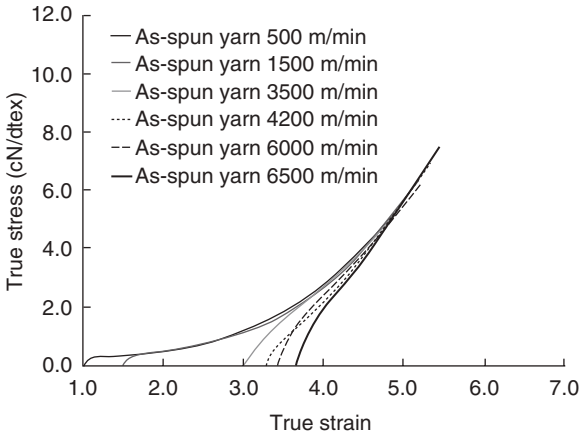

4.18 Shifted true stress–strain curves for undrawn nylon 6 yarns obtained at different wind-up speeds, as indicated in the legend.

4000 m/min, on the other hand, the shifted true stress–strain curves coincide with the mastercurve only in the final strain-hardening regime. This result indicates a change in network topology with increasing wind-up speed. Based on a detailed structural investigation of nylon 6 yarns, it has been found that a transition in structure-formation mechanism occurs at wind-up speeds of about 3000 m/min, associated with the onset of spin line crystallization.

Below 3000 m/min, the as-spun nylon 6 is largely amorphous. It starts to develop crystallinity at above this speed. The crystals developed during spinning are primarily γ. At higher speed, more crystallization takes place. The partially crystallized filament yarn with γ crystals, on conditioning, develops additional α crystallinity (post-crystallization). As the speed of spinning is increased, content of γ crystals increases while that of α crystals decreases due to higher crystallization during spinning and limited post-crystallization. At spinning speeds of 5500 m/min or above, the sample has mostly γ crystals. The effect of spinning speeds on birefringence profile and temperature profile of the spinning fiber is depicted in Figure 4.19.

The structure of the as-spun filaments depends markedly on spinning speed (take-up velocity) and on molecular weight.[39] Although crystallinity and γ fraction both increase with increasing take-up velocity, these quantities show an intricate dependence on molecular weight. The crystallinity at high take-up velocity (~3000 m/min) decreases with increasing molecular weight. At low take-up velocity (~1000 m/min) the opposite trend is observed, with the high-molecular-weight polymer having the higher crystallinity. This crossover in the behavior of the crystallinity is attributed to the fact that increasing either take-up velocity or molecular weight increases the crystallization rate but the final attainable crystallinity decreases with increasing molecular weight. The crystallization rate of the spun filaments increases with increase in molecular weight.

The tensile properties of the filaments are strong functions of both take-up velocity and molecular weight. The initial modulus and tensile strength increase and elongation to break decrease with increase of take-up velocity or molecular weight. The true strength at fracture is also found to increase with increase of molecular weight.

4.17 Drawing and heat setting

The as-spun fibers have poor elasticity (inability to recover) and they undergo plastic deformation on application of low levels of stress. This makes them unsuitable for use in applications including that of apparel. The polymer chains in the as-spun fibres are in partially folded conformation and can extend easily on application of stresses. Figure 4.20 shows a stress–strain plot of an as-spun fiber. The elastic region is small and is bounded by the yield point that occurs at a low stress and extension level. Following the yield point, the fiber shows deformation without much resistance till all the chains are unfolded and a new improved (more elastic) network of polymer is formed. In this region, the polymer chains assume new extended conformation and do not recover back to their original state when stresses are released. This region is known as region of 'natural draw' and the extensibility is called 'natural draw ratio (NDR)' of the fibers. This

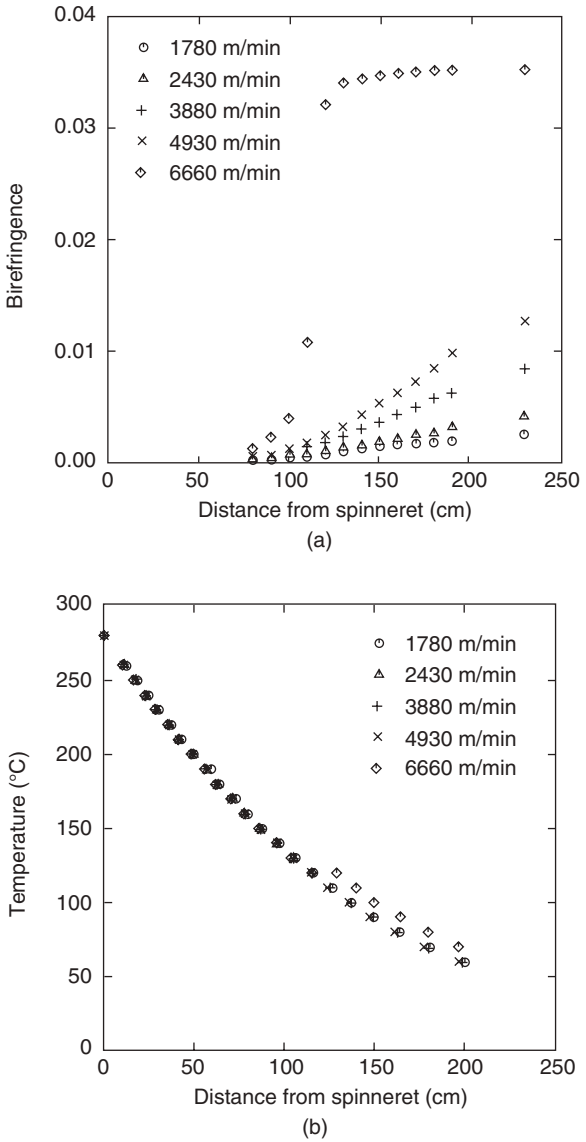

4.19 On-line experimental measurements for nylon 6 melt spun with a mass throughput of 2.99 g/min. (a) Birefringence profiles; (b) temperature profiles.

region of easy extensibility must be removed to make the fibers show the behavior of increasing resistance with increasing extension.

Drawing is necessary to remove the region of natural draw of the fibers. When the fiber is drawn beyond the NDR, polymer chains form an elastic network with extended conformation in the direction of draw (i.e. along

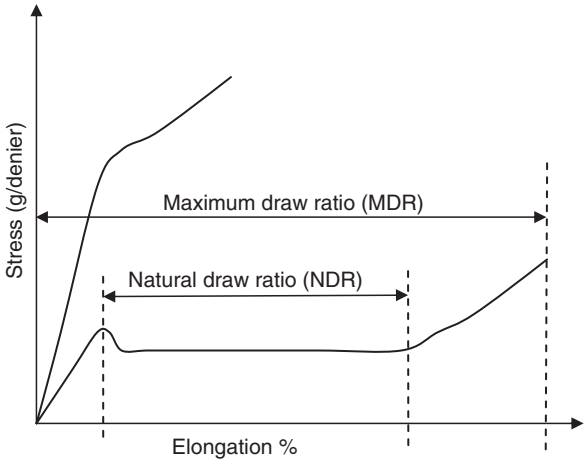

4.20 Stress–strain curves for as-spun and spun-drawn fibre.

the fiber axis). This gives fibers higher yield point, strength, initial modulus, and recovery compared to its as-spun form. Figure 4.20 also shows a typical stress–strain plot of a drawn fiber in comparison to that of an as-spun fiber. Maximum draw ratio (MDR), in contrast, is the maximum extensibility a fiber may be subjected to, before it breaks. The natural draw ratio in the as-spun fiber is a function of its spinning speed as discussed earlier.

The drawing is normally carried out by a cold drawing process where the fiber is drawn by forming a neck (also known as neck drawing). The location and stability of the neck is important in obtaining a uniformly drawn filament yarn. A snubbing pin may be used to help the formation of the neck or to stabilize it in a narrow zone. The drawing is carried out at just above the T_g of the polymer. For apparel grade nylon 6, drawing is carried out at room temperature.

Drawing may be carried out in a single step called single stage drawing as in apparel grade yarn or in two or more steps called two stage drawing or multistage drawing, as in high performance tire yarns. There are certain advantages of drawing the material in more than one stage such as reduced defects in drawn fiber due to partial relaxation of critical stresses during the drawing process. Drawing is normally carried out as a separate process on a separate machine as described above; however, at times, drawing may be combined with spinning machine to provide in-line drawing.

As stated earlier, in drawing, polymer chains are unfolded and oriented by applying an external tensile stress in the direction of the fiber axis. The level of applied stress depends upon the state of as-spun fiber, the draw ratio, the draw rate, the draw temperature and the moisture content of the fiber. Filaments undergo flow deformation drawing when drawn at either

a very low strain rate or at a high temperature. The filaments undergo a ductile failure when they are drawn at a high strain rate or at a low temperature. Therefore, in order to draw the filament in neck deformation, the rate and temperature of drawing must be optimized for a given fiber.

4.18 Mechanism of drawing in polyamides

The two theoretical schemes used for prediction of orientation from network deformation are (a) the affine and (b) pseudo-affine deformation mechanisms. In the affine scheme, network junctions are thought to be connected by flexible chains. Upon stretching, the network points are displaced in direct proportion to the macroscopic deformation. As a result, the rotatable 'random links' comprising the network chains will gradually adopt a more and more oriented configuration. In pseudo-affine deformation, on the other hand, the structural elements undergoing deformation are assumed to have no extensibility themselves but are rigid entities simply rotating in proportion to the macroscopic deformation of the sample.

The undrawn nylon 6 yarns are always partially crystalline, irrespective of the wind-up speed. The amorphous and crystalline orientation factors are plotted as a function of draw ratio in Figure 4.21.[40] The crystalline orientation factor fc initially increases sharply, leveling off at higher draw ratio whereas fa initially rises very slowly becoming important only at the highest draw ratios. It appears that the crystalline phase responds to draw ratio in a pseudo-affine fashion whereas the amorphous phase follows a rubber-like, affine deformation.[40] This result can be understood in

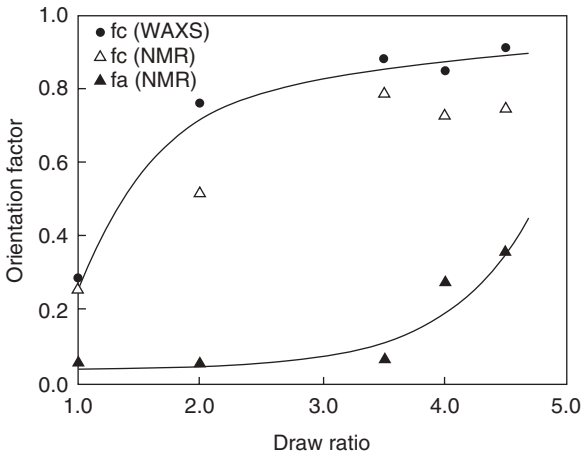

4.21 Crystalline and amorphous orientation factors fc and fa of drawn yarns as a function of draw ratio determined from WAXS and solid-state NMR measurements.

qualitative terms since crystallites act as rigid entities in the fiber structure whereas the amorphous phase consists of flexible chains, acting as a rubber network. Since the amorphous orientation is comparatively low at the maximum draw ratios, it is reasonable to assume that further drawing is hampered by the crystalline phase. This behavior of semicrystalline nylon is in contrast to drawing of as-spun PET, which is mostly amorphous and follows the affine deformation mechanism.

The crystalline structure of nylon 6 changes with the draw ratio at a given strain and temperature. This has been studied by measuring equatorial crystallinity index (ECI) with strain percentage as shown in Figure 4.22.[41] This behaviour of ECI on strain percentage may be separated into three distinct regimes: regime I (0–15% strain); regime II (15–100% strain); and regime III (100% strain and greater). In regime I, the gamma ECI decreases while both the alpha and total ECI increase. The majority of this increase occurs after the first extension, from 0 to 5% strain. The increase of the alpha ECI is always greater in magnitude than the decrease of the gamma ECI in this region; so the net result, the total ECI, is increasing as well. In the second regime the a-phase, g-phase, and total ECI are all decreasing. Finally, in the third regime the α-phase ECI remains constant and the γ-phase ECI drops to zero, thus forcing the total ECI to remain constant as well.

Since the increase of the a-phase ECI is greater than the decrease of the γ-phase ECI, a significant percentage of the α-phase increase must be due to conversion of the amorphous phase as opposed to the γ to α conversion. The decrease in the γ-phase ECI could be a result of two competing effects. Either the γ-phase is being converted to the α-phase, as discussed above, or the γ-phase crystals are being destroyed during the drawing process.

4.19 Heat setting

Annealing tends to increase the amount of α-phase mainly at the expense of the amorphous contribution. The nature of the α-phases changes; it becomes monoclinic and increases in perfection as the severity of annealing increases.[42] At low spin draw ratios there is very little γ-phase initially, but there is pseudohexagonal α-phase present (a*). As noted by Illers[5] and others[43,44,45], there is no difficulty in transforming this paracrystalline pseudohexagonal α to the monoclinic α form. In the high spin draw ratio samples containing appreciable γ-phase, there is a decrease in the relative amount of γ-phase on annealing, but γ-phase is not eliminated by the most severe annealing treatment investigated (2 h in boiling aqueous 20% formic acid solution). The low-SDR samples anneal more readily to the α-phase.[42]

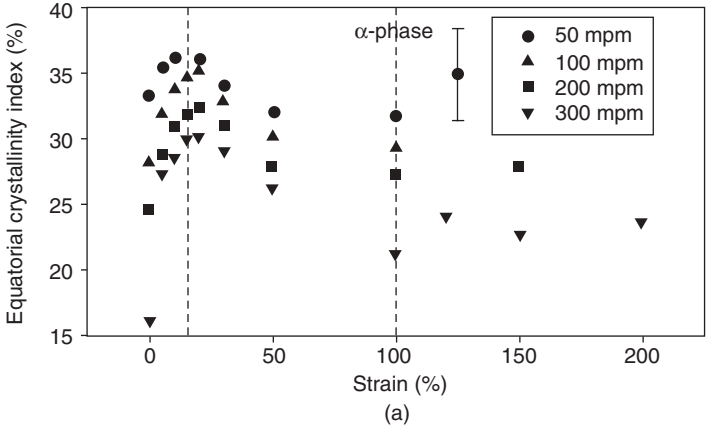

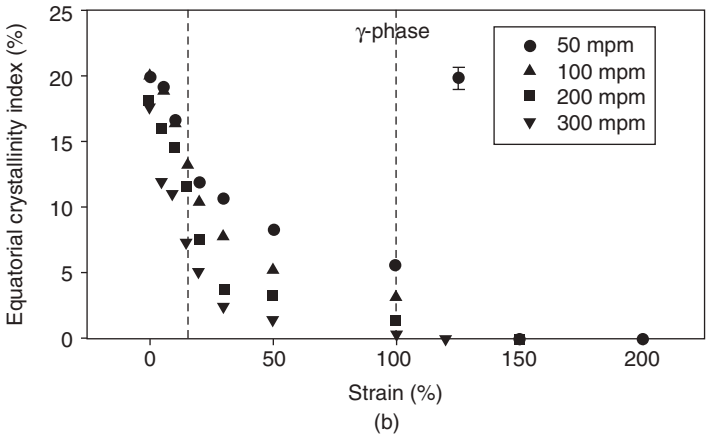

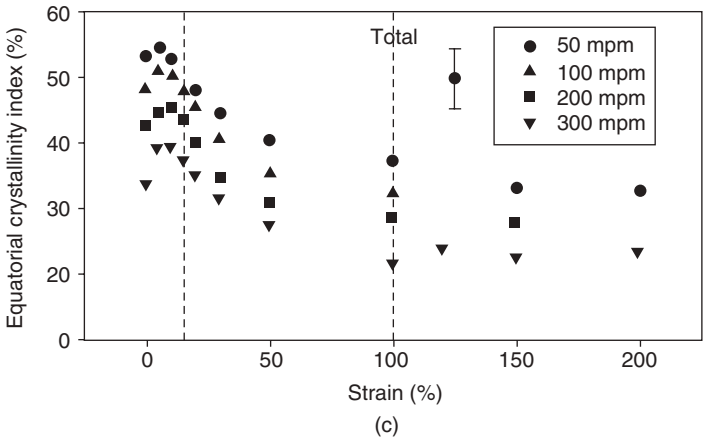

4.22 The equatorial crystallinity index (ECI) as a function of take-up speed and strain percentage of the: (a) α-phase; (b) γ-phase; and (c) total (α + γ); MPM = metres per minute.

4.20 References

1. MCINTYRE J. E., *Synthetic Fibres: Nylon, Polyester, Acrylic, Polyolefin*, Woodhead Publishing Limited, Cambridge, 2005.
2. REIMSCHUESSEL H. K., 'Nylon 6 Polymerization: Chemistry and Mechanism', *J Polym Sci Macromol Rev*, 1977, 12, 65.
3. ZIMMERMAN J., in *Encyclopedia of Polymer Science and Technology Vol. 11: Polyamides*, Interscience Publishers, New York, 1981, p. 331.
4. SWEENY W. and ZIMMERMAN J., in *Encyclopedia of Polymer Science and Technology, Volume 10*, (eds) N. M. Bikales and J. Conrad, John Wiley & Sons, New York, 1969.
5. FLORY P. J., 'Fundamental principles of condensation polymerization', *J Am Chem Soc*, 1946, 39, 137–97.
6. STEPPAN D. D., DOHERTY M. F. and MALONE M. F., 'A kinetic and equilibrium model for nylon 6,6 polymerization', *J Appl Polym Sci*, 1987, 33, 2333–44.
7. SUM W. M., (DU PONT), 'Polymerization of polyamide-forming reactants with hypophosphite catalysts', US Patent Office, Pat. No. 3,173,898, 1965.
8. SCHLACK P., (I. G. FARBEN), US Patent Office, Pat. No. 2,241,321, 1941.
9. GUPTA V. B. and KOTHARI V. K., *Manufactured Fibre Technology*, Chapman and Hall, London, 1997.
10. AGRAWAL A. K., DEVIKA K. and MANABE T., 'Simulation of hydrolytic polymerization of nylon-6 in industrial reactors: part i. mono-acid-stabilized systems in VK tube reactors', *Industrial & Engineering Chemistry Research*, 2001, 40(12), 2563–2572.
11. GUPTA S. K., NAIK C. D., TANDON P. and KUMAR A., 'Simulation of molecular weight distribution and cyclic oligomer formation in the polymerization of nylon 6', *J Appl Polym Sci*, 1981, 26(7), 2153–2163.
12. LAUN H. M., 'Viscoelastic behavior of nylon-6 melts', *Rheol. Acta*, 1979, 18, 478.
13. SRIVASTAVA, D. and GUPTA, S. K., Optimization of a tubular nylon-6 reactor with radial gradients. *Polym. Eng. Sci.* 1991, 31(8), 596–606.
14. GUPTA, S. K. and TJAHJADI, M., Simulation of an industrial nylon-6 tubular reactor, *J. Appl. Polym. Sci.* 1987, 33, 933–954.
15. AGRAWAL, A. K., DEVIKA K. and MANABE, T., 'Simulation of hydrolytic polymerisation of nylon-6 in industrial reactors: part 1. Monoacid stabilized systems in VK tube reactors', *Ind. Eng. Chem. Res.* 2001, 40, 2563–2572.
16. AGRAWAL, A. K., GUPTA, DEEPAK K. and DEVIKA K, 'Effect of diacid stabilizers on kinetics of hydrolytic polymerization of ε-caprolactam in industrial reactors', *J. Applied Polymer Science*, (2007), 104(4), 2065–2075.
17. FUKUMOTO, O. Equilibria between Polycapramide and Water. I. *J. Polym. Sci.* 1956, 22, 263–270.
18. B. R. RAO and K. V. DATYE, *Textile Chemist & Colourist*, 28(10), (1996) 17–24.
19. DATYE K. V., *Colourage*, February (1994) 7–12.
20. KARMAKAR S. R., BHATTACHARYYA K. and DEB T., *Colourage Annual*, (1996) 47–58.
21. VAIDYA A. A., NARRASIMHAN K. V. and AHUJA G., *Man made Textiles in India*, (1986), 29(5), 213–223, 250.

22. GUPTA V. B. and KOTHARI V. K. (Eds) *Manufactured Fibre Technology*, Chapman & Hall, London, 1st Edn, 1997, Chap 14.
23. BARASHKOV N. N., VYSOTSKII V. N. and GRIGOR'Y I. N., *Khim. Volokna*, (1987), 29(6) 38–39.
24. PETERS J., *ATI*, October (1987) 46–47.
25. GARVANSKA R., MINCHEVA I. and DIMOV K., *Khim. Ind. (Sofia)* (1982) No. 6, 261–263, *Chem. Abstr.*, 98(1983), No. (6 35941).
26. CAZZARO G. and THOMPSON R., *Textile Asia*, December (1989), 80–86.
27. RIDGWAY J. S., *J. Appl. Polym. Sci.,* (1988) 35(1), 215–227.
28. KASE, S. and MATSUO, T. *Journal of Applied Polymer Science*, v 11 (1967) 251.
29. JEFFER S. DENTON, JOHN A. CUCUL and PAUL A. Tucker, 'Computer simulation of high-speed spinning of poly(ethyleneterephthalate)', *Journal of Applied Polymer Science*, 1995, 57, 939–951.
30. ANTONIOS K. DOUFAS, ANTHONY J. MCHUGH and CHESTER MILLER, 'Simulation of melt spinning including flow-induced crystallization Part I. Model development and predictions', *J. Non-Newtonian Fluid Mech.*, 2000, 92, 27–66.
31. JUNG S. KIM and SANG Y. KIM, 'Necking behavior in high-speed melt spinning of poly(ethylene terephthalate)', *Journal of Applied Polymer Science*, 2000, 76, 446–456.
32. MCHUGH A. J. and DOUFAS A. K., 'Modeling flow-induced crystallization in fibre spinning', Composites: Part A, *Applied Science and Manufacturing*, 2001, 32, 1059–66.
33. ANTONIOS K. DOUFAS, ANTHONY J. MCHUGH, CHESTER MILLER and ARAVIND IMMANENI, 'Simulation of melt spinning including flow-induced crystallization Part II. Quantitative comparisons with industrial spinline data', *J. Non-Newtonian Fluid Mech.*, 2000, 92, 81–103.
34. RAJEN M. PATEL, JAYENDRA H. BHEDA and JOSEPH E. SPRUIELL, 'Dynamics and structure development during high-speed melt spinning of nylon 6. II. Mathematical modeling', *Journal of Applied Polymer Science*, 1991, 42, 1671–1682.
35. TAKESHI KIKUTANI, YUTAKA KAWAHARA, NAOKI OGAWA and NORIMASA OKUI, 'Capturing of real image of neck-like deformation from high-speed melt spinning line', *Sen-I Gakkaishi*, 1994, 50(12), 561–566.
36. JIRO SHIMIZU and TAKESHI KIKUTANI, 'Dynamics and evolution of structure in fibre extrusion', *Journal of Applied Polymer Science*, 202, 83, 539–558.
37. J. H. BHEDA and J. E. SPRUIELL, *Journal of Applied Polymer Science*, Vol. 39, 447–463 (1990).
38. DEOPURA B. L. and MUKHERJEE A. K., 'Nylon 6 and nylon 66 fibers', in *Manufactured Fibre Technology* (Eds) V. B. Gupta and V. K. Kothari, Chapman & Hall: London, 1997, 318–356.
39. KOYAMA K., SURYADEVARA J. and SPURIELL J. E., *Journal of Applied Polymer Science*, Vol. 31, 2203–2229 (1986).
40. PENNING J. P., VAN RUITEN J., BROUWER R. and GABRIËLSE W., 'Orientation and structure development in melt-spun Nylon-6 fibres', *Polymer* 44 (2003) 5869–5876.
41. SAMON J. M., SCHULTZ J. M. and HSIAO B. S., 'Study of the cold drawing of nylon 6 fiber by in-situ simultaneous small- and wide-angle X-ray scattering techniques', *Polymer* 41 (2000) 2169–2182.

42. GIANCHANDANI J., SPRUIELL J. E. and CLARK E. S., *Journal of Applied Polymer Science*, Vol. 27, 3527–3551 (1982).
43. ILLERS H. K., HABERKORN H. and SINAK P., *Makromol. Chem.*, 158, 285 (1972).
44. STEPANIAK R. F., GARTON A., CARLSSON D. J. and WILES D. M., *J. Polym. Sci., Polym. Phyi. Ed.*, 17, 987 (1979); also *J. Appl. Polym. Sci.*, 23, 1747 (1979).
45. BANKAR V. G., SPRUIELL J. E., and WHITE J. L., *J. Appl. Polym. Sci.*, 21, 2341 (1977).